A New Multilayer Nonhydrostatic Formulation for Surface Water Waves

Gang Wang[†,*], Qiuhua Liang[‡], Jinhai Zheng[†] and Peng Wan[†]

[†]Key Laboratory of Coastal Disaster and Defence (Hohai University), Ministry of Education, Nanjing, China

[‡]School of Civil Engineering and Geosciences, Newcastle University, Newcastle upon Tyne, United Kingdom

LRH: Wang *et al.*

RRH: New Multilayer Nonhydrostatic Formulation

ABSTRACT

This work presents a new multilayer nonhydrostatic formulation for surface water waves. The new governing equations define velocities and pressure at an arbitrary location of a vertical layer and only contain spatial derivatives of maximum second-order. Stoke-type Fourier and shoaling analyses are carried out to scrutinize the mathematical properties of the new formulation, subsequently optimizing the representative interface and the location to define variables in each layer to improve model accuracy. Following the analysis, the one-layer model exhibits accurate linear and nonlinear characteristics up to $kd = \pi$, demonstrating similar solution accuracy to the existing second-order Boussinesq-type models. The two-layer model with optimized coefficients can maintain its linear and nonlinear accuracy up to $kd = 4\pi$, which boasts of better solution accuracy a larger application range than most of the existing fourth-order Boussinesq model and two-layer Boussinesq models. The three-layer model presents accurate linear and nonlinear characteristics up to $kd = 10\pi$, effectively removing any shallow water limitation. The current multilayer nonhydrostatic water wave model does not predefine the vertical flow structures and

[*] Corresponding author: gangwang@hhu.edu.cn

more accurate vertical velocity distributions can be obtained by taking into account the velocity profiles in coefficient optimization.

ADDITIONAL INDEX WORDS: *Nonhydrostatic Modeling*, *Multilayer Model*, *Wave Propagation*, *Surface Gravity Waves*

INTRODUCTION

Coastal engineers and researchers develop mathematical and numerical models to simulate different types of water waves for engineering applications, from initiation, propagation from deep to shallow water, breaking in nearshore zone to run-up on the beach. For shallow waves with wavelength much greater than water depth, the water motion is predominantly horizontal and propagates at the same speed with negligible vertical acceleration, satisfying the hydrostatic pressure assumption. This leads to the shallow wave theory as described by the shallow water equations. However, outside of the nearshore zones where water becomes deeper, the wave dispersion effects become significant; waves of different frequencies propagate at different phase speed and can no longer be accurately described by the shallow water equations. Therefore, the shallow water equations only support limited applications in coastal engineering.

Through incorporating more frequency dispersion and nonlinearity effects to the non-dispersive shallow-water theory, Boussinesq-type equations provide a more robust mathematical model for wave propagation in coastal regions (Brocchini, 2013). Peregrine (1967) pioneered the derivation of the Boussinesq equations with a variable water depth using the depth-averaged velocity as a dependent variable. This classical Boussinesq formulation includes only the lowest-order frequency dispersion and nonlinearity effects, and is only applicable to relatively shallow water. A number of attempts have been made to extend the applicability of Boussinesq equations to deeper water. Madsen and Sørensen (1992) presented a set of improved Boussinesq equations by including extra high-order terms to better describe wave dispersion and shoaling. Nwogu (1993) derived an alternative set of Boussinesq equations using the velocity at an arbitrary water level as an independent variable to allow applications in deeper water.

Gobbi, Kirby and Wei (2000) adopted a fourth-order polynomial to approximate the vertical flow distribution (alternative equations generally used quadratic polynomial approximation), retaining more nonlinear and dispersive terms in the Boussinesq equations to improve their application range. Lynett and Liu (2004a) proposed a set of multilayer Boussinesq equations by approximating the vertical flow field in each layer with quadratic polynomials; the equations present good linear and nonlinear behavior although the highest order of spatial differentiation is only less than three, leading to simple numerical discretization. More Boussinesq-type equations have been reported in literature, which usually follow a similar approach to one of the above models (Liu and Fang, 2015; Madsen and Schaffer, 1998). Clearly, the improved accuracy of the Boussinesq equations comes at a price of more sophisticated formulation (Agnon, Madsen and Schaffer, 1999; Madsen, Bingham and Liu, 2002; Madsen, Bingham and Schaffer, 2003), demanding complicated numerical schemes to resolve the higher-order derivative terms and also high computational cost.

Theoretically, a numerical model solving the fully 3D hydrodynamic equations, *e.g.* the Euler equations or the Navier-Stokes equations, can accurately represent a full range of wave phenomena from deep to shallow water. The main challenge in discretizing these fully 3D equations to predict free-surface wave motions is to accurately capture the moving free surface which is part of the solution itself. A number of techniques have been developed for this purpose, including the volume of fluid (VOF) method (Hirt and Nichols, 1981; Lin and Liu, 1998), Lagrangian-Eulerian method (Silva Santos and Greaves, 2007) and level set methods (Osher and Fedkiw, 2001). Some of these approaches can also handle sharp-fronted free surface and wave overturning. However, these surface-capturing approaches are commonly computationally demanding, prohibiting their wider application to large-scale wave climate prediction. In case where the free surface can be assumed to be continuous and featured as a single value function of the horizontal plane, simplified numerical methods can be employed to solve the 3D governing equations to reduce computational cost. These models typically involve decomposition of the pressure terms into hydrostatic and non-hydrostatic components, and are known as non-hydrostatic models.

In developing non-hydrostatic models, a key challenge is to impose the pressure boundary condition at the free surface and resolve the non-hydrostatic terms, which plays an important role in providing accurate description of wave dispersion. When developing their 3D quasi-hydrostatic model, Casulli and Stelling (1998) assumed hydrostatic pressure distribution at the top layer of the vertical dimension; a large number of vertical layers are required to provide meaningful solutions for short waves. Stelling and Zijlema (2003) subsequently implemented the Keller-box method to approximate the non-hydrostatic pressure terms; the resulting model can accurately capture the wave characteristics with one or two vertical layers, leading to much improved computational efficiency. To obtain the free surface boundary condition, Yuan and Wu (2004) derived non-hydrostatic pressure at the top layer by integrating the vertical momentum equation from the center of the layer to the moving free surface, providing increased phase accuracy for the simulation of dispersive waves. Ahmadi, Badiei and Namin (2007) proposed a new implicit approach to treat the non-hydrostatic pressure at the top layer, releasing the model from any hydrostatic pressure assumption across the entire water column and giving improved solution accuracy for free surface elevation and wave celerity. Young and Wu (2009) reported an effective approach to obtain the analytical pressure distribution at the top layer by introducing Boussinesq-like equations into their implicit non-hydrostatic model. Later on, Choi, Wu and Young (2011) presented an efficient curvilinear non-hydrostatic model for surface water waves using a higher order (either quadratic or cubic spline function) integral method for the top-layer non-hydrostatic pressure within a staggered grid framework. Most of these non-hydrostatic models discretize the vertical domain into uniform layers; the number of layers required for a specific application is usually determined through trial and error.

Considering the fact that the velocity and non-hydrostatic pressure are predominant near the free surface, non-uniform vertical discretization, *i.e.* with finer resolution layers on the top, may be used to improve the model capability in describing wave dispersion. This strategy was adopted by Yuan and Wu (2006) to develop their 3D implicit surface-wave model. Zhu, Chen and Wan (2014) introduced an approach to achieve optimal distribution of vertical layers by considering the analytical dispersion relationship of a non-hydrostatic Euler water wave model.

Mostly based on direct discretization of the Euler equations or the Navier-Stokes equations, the non-hydrostatic models have been widely used for the simulation of wave propagation from deep water to the surf zone. It is difficult to analyze the accuracy for these models, which is dependent on the use of different vertical layers and different numerical methods. There still lacks of a comprehensive theoretical framework to precisely determine the application range of a model. Preliminary attempt was made by Bai and Cheung (2013) to derive a new multilayer formulation by integrating the continuity and Euler equations over each layer and specify its application range through analysis of wave dispersion and nonlinearity.

It is evident that 1) specifying the pressure especially at the top-layer and 2) using the non-uniform vertical layers can significantly improve the nonhydrostatic models' capability to describe wave dispersion and nonlinearity characteristics. This paper combines these two strategies to derive a new set of multilayer nonhydrostatic formulations from the Euler equations. To balance the benefit of using lower-order derivatives and the desire of achieving high accuracy of linearity and nonlinearity, the pressure and velocities are approximated as quadratic polynomials using the Taylor expansions. Different from the aforementioned existing models that define the variables at the center or at the edge of a layer, the current model defines the pressure and velocities at an arbitrary level within a layer. As the fluid can be assumed inviscid and incompressible, the irrotationality condition is reinforced to simplify the fluid dynamics equations. The new formulation involves only the first- and second-order spatial derivatives, which can be solved using simpler numerical methods. Systematic analysis of dispersion and nonlinearity is further performed to evaluate the merits and limitations of the new formulation. The thicknesses of layers and the position of flow variables at each layer are finally determined by minimizing the linearity and errors in comparison with Stokes theory.

The rest of the paper is organized as follows: the next section briefly reviews the continuity and Euler equations for describing free-surface fluid motions. The third section present detailed derivation of the new formulation; the fourth section discusses the linearity and nonlinearity characteristics of the new formulation for up to three layers; and finally, conclusions are drawn in the last section.

METHODS

Euler equations are chosen as the governing equations for surface water waves. velocities and pressure are defined at an arbitrary location of each vertical layer, and a new multilayer nonhydrostatic formulation is detailed derived.

Governing Equations

The current work focuses on surface gravity waves, including wind waves, swell and tsunamis, and so the variation of water density is insignificant over the temporal and spatial scales for most of the engineering applications, leading to incompressible flows. Also, for wave propagation over a large spatial scale, the velocity gradient is relatively small; the vortices are usually weak; and so the viscous effect becomes negligible. The inviscid and incompressible fluid assumptions lead to irrotational flows and the flow dynamics may be described by the Euler equations based on momentum conservation

$$\frac{\partial u}{\partial t}+u\frac{\partial u}{\partial x}+v\frac{\partial u}{\partial y}+w\frac{\partial u}{\partial z}=-g\frac{\partial \zeta}{\partial x}-\frac{1}{\rho}\frac{\partial q}{\partial x} \tag{1}$$

$$\frac{\partial v}{\partial t}+u\frac{\partial v}{\partial x}+v\frac{\partial v}{\partial y}+w\frac{\partial v}{\partial z}=-g\frac{\partial \zeta}{\partial y}-\frac{1}{\rho}\frac{\partial q}{\partial y} \tag{2}$$

$$\frac{\partial w}{\partial t}+u\frac{\partial w}{\partial x}+v\frac{\partial w}{\partial y}+w\frac{\partial w}{\partial z}=-\frac{1}{\rho}\frac{\partial q}{\partial z} \tag{3}$$

and the continuity equation based on mass conservation

$$\frac{\partial u}{\partial x}+\frac{\partial v}{\partial y}+\frac{\partial w}{\partial z}=0 \tag{4}$$

where t denotes the time; x, y and z represent the 3D Cartesian coordinates; u, v and w are the velocity components in the three coordinate directions; ζ is the free surface elevation above the still water level; $h = \zeta + d$ defines the total flow depth with d being the still water depth; g and ρ are respectively the acceleration due to gravity and fluid density; q is the non-hydrostatic pressure components and consequently the total pressure p is given by

$$p = \rho g(\zeta - z) + q \tag{5}$$

where $\rho g(\zeta - z)$ calculates the hydrostatic pressure. Due to the irrotational fluid assumption, Eqs. (1-4) satisfy the following conditions

$$\frac{\partial u}{\partial z} = \frac{\partial w}{\partial x}, \frac{\partial v}{\partial z} = \frac{\partial w}{\partial y}, \frac{\partial u}{\partial y} = \frac{\partial v}{\partial x} \tag{6}$$

For water wave simulations, the dynamic and kinematic boundary conditions must also be satisfied at the free surface, *i.e.*

$$q = 0 \qquad \text{at } z = \zeta \tag{7}$$

$$w = \frac{\partial \zeta}{\partial t} + u\frac{\partial \zeta}{\partial x} + v\frac{\partial \zeta}{\partial y} \qquad \text{at } z = \zeta \tag{8}$$

Assuming a rigid and impermeable bed, the no-flux boundary condition is given by

$$w\big|_{z=-d} = -u\frac{\partial d}{\partial x} - v\frac{\partial d}{\partial y} \tag{9}$$

New Multilayer Wave Equations

The water column is divided into N vertical layers by $(N - 1)$ non-intersecting interfaces between the bottom and the free surface, as shown in Figure 1, with an arbitrary interface located at

$$z_j = -\alpha_j d \tag{10}$$

where $1 = \alpha_1 > \alpha_2 \ldots \alpha_{j-1} > \alpha_j > \alpha_{j+1} \ldots > \alpha_{N-1} \geq 0$. The vertical layers are not necessary to be uniform. The free surface defines the upper interface of the top layer and is time-independent. Theoretically, the upper and lower interfaces of the top layer may intersect under severe wave conditions, leading to unphysical solutions. To avoid this, it is required that the thickness of the top layer must be at least larger than the wave amplitude. In applications, it is recommended that the thickness of the top layer should be set conservatively larger than the wave height, taking into account the shoaling effect in shallow water. This restricts the use of excessive number of vertical layers to improve model accuracy; but it will not pose much restriction on actual applications as the current formulation is derived to accurately describe wave propagation with fewer layers. More details will be provided in the following sections.

The flow variables, *i.e.* velocities and pressure, can be defined at an arbitrary elevation h_j within a vertical layer j, where

$$h_j = -\beta_j d \tag{11}$$

and $\alpha_{j-1} \geq \beta_j \geq \alpha_j$.

Herein it intends to develop a new mathematical model to flexibly describe the wave motions from deep to shallow water zones. Even in the deep water, the vertical variation of the water motions in each layer will be weak and predominantly horizontal. Subsequently, the velocities at an arbitrary point within layer j may be expanded using a Taylor series with respect to h_j:

$$u = u_j + \left(z - h_j\right)\left(\frac{\partial u}{\partial z}\right)_j + \frac{\left(z - h_j\right)^2}{2}\left(\frac{\partial^2 u}{\partial z^2}\right)_j + \cdots \tag{12}$$

Using the irrotationality condition (6), the above equation can be written as

$$u = u_j + \left(z - h_j\right)\left(\frac{\partial w}{\partial x}\right)_j + \frac{\left(z - h_j\right)^2}{2}\frac{\partial}{\partial z}\left(\frac{\partial w}{\partial x}\right)_j + \cdots \tag{13}$$

Using the continuity equation Eq.(4), it can be further rewritten as

$$u = u_j + \left(z - h_j\right)\left(\frac{\partial w}{\partial x}\right)_j - \frac{\left(z - h_j\right)^2}{2}\left(\frac{\partial^2 u}{\partial x^2} + \frac{\partial^2 u}{\partial y^2}\right)_j + \cdots \tag{14}$$

Similarly, the expressions for the horizontal velocity component v and the vertical velocity component w can be obtained, *i.e.*

$$v = v_j + \left(z - h_j\right)\left(\frac{\partial w}{\partial y}\right)_j - \frac{\left(z - h_j\right)^2}{2}\left(\frac{\partial^2 v}{\partial x^2} + \frac{\partial^2 v}{\partial y^2}\right)_j + \cdots \tag{15}$$

and

$$w = w_j - \left(z - h_j\right)\left(\frac{\partial u}{\partial x} + \frac{\partial v}{\partial y}\right)_j - \frac{\left(z - h_j\right)^2}{2}\left(\frac{\partial^2 w}{\partial x^2} + \frac{\partial^2 w}{\partial y^2}\right)_j + \cdots \tag{16}$$

The partial derivatives in Eqs. (14) ~ (16) may be expressed using the variables at the elevation h_j. The first-order derivatives thus become

$$\left(\frac{\partial w}{\partial x}\right)_j = \frac{\partial w_j}{\partial x} + \frac{\partial h_j}{\partial x}\left(\frac{\partial u}{\partial x} + \frac{\partial v}{\partial y}\right)_j + \cdots \tag{17}$$

$$\left(\frac{\partial w}{\partial y}\right)_j = \frac{\partial w_j}{\partial y} + \frac{\partial h_j}{\partial y}\left(\frac{\partial u}{\partial x} + \frac{\partial v}{\partial y}\right)_j + \cdots \tag{18}$$

$$\left(\frac{\partial u}{\partial x}\right)_j = \frac{\partial u_j}{\partial x} - \frac{\partial h_j}{\partial x}\left(\frac{\partial w}{\partial x}\right)_j + \cdots \tag{19}$$

$$\left(\frac{\partial v}{\partial y}\right)_j = \frac{\partial v_j}{\partial y} - \frac{\partial h_j}{\partial y}\left(\frac{\partial w}{\partial y}\right)_j + \cdots \tag{20}$$

which can lead to

$$\left(\frac{\partial w}{\partial x}\right)_j = \frac{\partial w_j}{\partial x} + \frac{\partial h_j}{\partial x}\left(\frac{\partial u_j}{\partial x} + \frac{\partial v_j}{\partial y}\right) + O\left[\left(\frac{\partial h_j}{\partial x}\right)^2, \frac{\partial h_j}{\partial x}\frac{\partial h_j}{\partial y}, \left(\frac{\partial h_j}{\partial y}\right)^2\right] \tag{21}$$

$$\left(\frac{\partial w}{\partial y}\right)_j = \frac{\partial w_j}{\partial y} + \frac{\partial h_j}{\partial y}\left(\frac{\partial u_j}{\partial x} + \frac{\partial v_j}{\partial y}\right) + O\left[\left(\frac{\partial h_j}{\partial x}\right)^2, \frac{\partial h_j}{\partial x}\frac{\partial h_j}{\partial y}, \left(\frac{\partial h_j}{\partial y}\right)^2\right] \tag{22}$$

$$\left(\frac{\partial u}{\partial x}\right)_j = \frac{\partial u_j}{\partial x} - \frac{\partial h_j}{\partial x}\frac{\partial w_j}{\partial x} + O\left[\left(\frac{\partial h_j}{\partial x}\right)^2\right] \tag{23}$$

$$\left(\frac{\partial u}{\partial y}\right)_j = \frac{\partial u_j}{\partial y} - \frac{\partial h_j}{\partial y}\frac{\partial w_j}{\partial y} + O\left[\left(\frac{\partial h_j}{\partial y}\right)^2\right] \tag{24}$$

$$\left(\frac{\partial v}{\partial x}\right)_j = \frac{\partial v_j}{\partial x} - \frac{\partial h_j}{\partial x}\frac{\partial w_j}{\partial x} + O\left[\left(\frac{\partial h_j}{\partial x}\right)^2\right] \tag{25}$$

$$\left(\frac{\partial v}{\partial y}\right)_j = \frac{\partial v_j}{\partial y} - \frac{\partial h_j}{\partial y}\frac{\partial w_j}{\partial y} + O\left[\left(\frac{\partial h_j}{\partial y}\right)^2\right] \tag{26}$$

In the above derivation, the products of the horizontal bottom gradients are neglected, and therefore the resulting formulation is restricted to the applications with slowly varying bottom.

Similarly, the second-order derivatives are rewritten as

$$\left(\frac{\partial^2 w}{\partial x^2}\right)_j = \frac{\partial^2 w_j}{\partial x^2} + O\left[\left(\frac{\partial h_j}{\partial x}\right)^2, \frac{\partial^2 h_j}{\partial x^2}\right] \tag{27}$$

$$\left(\frac{\partial^2 w}{\partial y^2}\right)_j = \frac{\partial^2 w_j}{\partial y^2} + O\left[\left(\frac{\partial h_j}{\partial y}\right)^2, \frac{\partial^2 h_j}{\partial y^2}\right] \tag{28}$$

$$\left(\frac{\partial^2 u}{\partial x^2}\right)_j = \frac{\partial^2 u_j}{\partial x^2} + O\left[\left(\frac{\partial h_j}{\partial x}\right)^2, \frac{\partial^2 h_j}{\partial x^2}\right] \tag{29}$$

$$\left(\frac{\partial^2 u}{\partial y^2}\right)_j = \frac{\partial^2 u_j}{\partial y^2} + O\left[\left(\frac{\partial h_j}{\partial y}\right)^2, \frac{\partial^2 h_j}{\partial y^2}\right] \tag{30}$$

$$\left(\frac{\partial^2 v}{\partial x^2}\right)_j = \frac{\partial^2 v_j}{\partial x^2} + O\left[\left(\frac{\partial h_j}{\partial x}\right)^2, \frac{\partial^2 h_j}{\partial x^2}\right] \tag{31}$$

$$\left(\frac{\partial^2 v}{\partial y^2}\right)_j = \frac{\partial^2 v_j}{\partial y^2} + O\left[\left(\frac{\partial h_j}{\partial y}\right)^2, \frac{\partial^2 h_j}{\partial y^2}\right] \tag{32}$$

where the second-order bottom effects and products of the first-order bottom gradients are neglected.

The velocities at an arbitrary point within layer j can thus be expressed as

$$\begin{aligned} u = u_j + \left(z - h_j\right)\left[\frac{\partial w_j}{\partial x} + \frac{\partial h_j}{\partial x}\left(\frac{\partial u_j}{\partial x} + \frac{\partial v_j}{\partial y}\right)\right] - \frac{\left(z - h_j\right)^2}{2}\left(\frac{\partial^2 u_j}{\partial x^2} + \frac{\partial^2 u_j}{\partial y^2}\right) \\ + O\left[\left(\frac{\partial h_j}{\partial x}\right)^2, \frac{\partial h_j}{\partial x}\frac{\partial h_j}{\partial y}, \left(\frac{\partial h_j}{\partial y}\right)^2, \frac{\partial^2 h_j}{\partial x^2}, \frac{\partial^2 h_j}{\partial y^2}\right] \end{aligned} \tag{33}$$

$$\begin{aligned} v = v_j + \left(z - h_j\right)\left[\frac{\partial w_j}{\partial y} + \frac{\partial h_j}{\partial y}\left(\frac{\partial u_j}{\partial x} + \frac{\partial v_j}{\partial y}\right)\right] - \frac{\left(z - h_j\right)^2}{2}\left(\frac{\partial^2 v_j}{\partial x^2} + \frac{\partial^2 v_j}{\partial y^2}\right) \\ + O\left[\left(\frac{\partial h_j}{\partial x}\right)^2, \frac{\partial h_j}{\partial x}\frac{\partial h_j}{\partial y}, \left(\frac{\partial h_j}{\partial y}\right)^2, \frac{\partial^2 h_j}{\partial x^2}, \frac{\partial^2 h_j}{\partial y^2}\right] \end{aligned} \tag{34}$$

$$\begin{aligned} w = w_j - \left(z - h_j\right)\left(\frac{\partial u_j}{\partial x} + \frac{\partial v_j}{\partial y} - \frac{\partial h_j}{\partial x}\frac{\partial w_j}{\partial x} - \frac{\partial h_j}{\partial y}\frac{\partial w_j}{\partial y}\right) - \frac{\left(z - h_j\right)^2}{2}\left(\frac{\partial^2 w_j}{\partial x^2} + \frac{\partial^2 w_j}{\partial y^2}\right) \\ + O\left[\left(\frac{\partial h_j}{\partial x}\right)^2, \left(\frac{\partial h_j}{\partial y}\right)^2, \frac{\partial^2 h_j}{\partial x^2}, \frac{\partial^2 h_j}{\partial y^2}\right] \end{aligned} \tag{35}$$

The Taylor series expansion may be also applied to the nonhydrostatic pressure, leading to

$$q = q_j + \left(z - h_j\right)\left(\frac{\partial q}{\partial z}\right)_j + \frac{\left(z - h_j\right)^2}{2}\left(\frac{\partial^2 q}{\partial z^2}\right)_j + \cdots \tag{36}$$

Substituting the vertical momentum Eq. (3) into the above equation yields

$$\begin{aligned} q = q_j &- \rho\left(z - h_j\right)\left[\left(\frac{\partial w}{\partial t}\right)_j + u_j\left(\frac{\partial w}{\partial x}\right)_j + v_j\left(\frac{\partial w}{\partial y}\right)_j + w_j\left(\frac{\partial w}{\partial z}\right)_j\right] \\ &- \rho\frac{\left(z - h_j\right)^2}{2}\frac{\partial}{\partial z}\left(\frac{\partial w}{\partial t} + u\frac{\partial w}{\partial x} + v\frac{\partial w}{\partial y} + w\frac{\partial w}{\partial z}\right)_j + \cdots \end{aligned} \tag{37}$$

Substitution of the continuity Eq. (4) into the above expression gives

$$\begin{aligned} q &= q_j - \rho\left(z - h_j\right)\left[\frac{\partial w_j}{\partial t} + u_j\left(\frac{\partial w}{\partial x}\right)_j + v_j\left(\frac{\partial w}{\partial y}\right)_j - w_j\left(\frac{\partial u}{\partial x}\right)_j - w_j\left(\frac{\partial v}{\partial y}\right)_j\right] \\ &\quad - \rho\frac{\left(z - h_j\right)^2}{2}\frac{\partial}{\partial z}\left(\frac{\partial w}{\partial t} + u\frac{\partial w}{\partial x} + v\frac{\partial w}{\partial y} - w\frac{\partial u}{\partial x} - w\frac{\partial v}{\partial y}\right)_j + \cdots \\ &= q_j - \rho\left(z - h_j\right)\left[\frac{\partial w_j}{\partial t} + u_j\left(\frac{\partial w}{\partial x}\right)_j + v_j\left(\frac{\partial w}{\partial y}\right)_j - w_j\left(\frac{\partial u}{\partial x}\right)_j - w_j\left(\frac{\partial v}{\partial y}\right)_j\right] \\ &\quad + \rho\frac{\left(z - h_j\right)^2}{2}\left\{\begin{aligned} &+\left(\frac{\partial^2 u}{\partial t\partial x}\right)_j + \left(\frac{\partial^2 v}{\partial t\partial y}\right)_j - \left(\frac{\partial u}{\partial z}\frac{\partial w}{\partial x}\right)_j + u_j\left(\frac{\partial^2 u}{\partial x^2} + \frac{\partial^2 v}{\partial x\partial y}\right)_j - \left(\frac{\partial v}{\partial z}\frac{\partial w}{\partial y}\right)_j \\ &+v_j\left(\frac{\partial^2 u}{\partial y\partial x} + \frac{\partial^2 v}{\partial y^2}\right)_j - \left(\frac{\partial u}{\partial x} + \frac{\partial v}{\partial y}\right)_j^2 + w_j\left(\frac{\partial^2 u}{\partial x\partial z}\right)_j + w_j\left(\frac{\partial^2 v}{\partial y\partial z}\right)_j \end{aligned}\right\} + \cdots \end{aligned} \tag{38}$$

Using the irrotationality condition in Eq. (6), the nonhydrostatic pressure at an arbitrary point within layer j can be finally expressed as

$$\begin{aligned} q = q_j &- \rho\left(z - h_j\right)\left[\left(\frac{\partial w}{\partial t}\right)_j + u_j\left(\frac{\partial w}{\partial x}\right)_j + v_j\left(\frac{\partial w}{\partial y}\right)_j - w_j\left(\frac{\partial u}{\partial x}\right)_j - w_j\left(\frac{\partial v}{\partial y}\right)_j\right] \\ &+ \rho\frac{\left(z - h_j\right)^2}{2}\left\{\begin{aligned} &\left(\frac{\partial^2 u}{\partial t\partial x}\right)_j + \left(\frac{\partial^2 v}{\partial t\partial y}\right)_j - \left(\frac{\partial w}{\partial x}\right)_j^2 - \left(\frac{\partial w}{\partial y}\right)_j^2 - \left(\frac{\partial u}{\partial x} + \frac{\partial v}{\partial y}\right)_j^2 \\ &+u_j\left(\frac{\partial^2 u}{\partial x^2} + \frac{\partial^2 v}{\partial x\partial y}\right)_j + v_j\left(\frac{\partial^2 u}{\partial y\partial x} + \frac{\partial^2 v}{\partial y^2}\right)_j + w_j\left(\frac{\partial^2 w}{\partial x^2} + \frac{\partial^2 w}{\partial y^2}\right)_j \end{aligned}\right\} + \cdots \end{aligned} \tag{39}$$

which may be further expressed in terms of the variables at the elevation h_j, *i.e.*

$$
\begin{aligned}
q = q_j - \rho\left(z-h_j\right) & \left[\begin{array}{l} \dfrac{\partial w_j}{\partial t} + u_j\dfrac{\partial w_j}{\partial x} + v_j\dfrac{\partial w_j}{\partial y} - w_j\left(\dfrac{\partial u_j}{\partial x} + \dfrac{\partial v_j}{\partial y}\right) \\ + \left(u_j\dfrac{\partial h_j}{\partial x} + v_j\dfrac{\partial h_j}{\partial y}\right)\left(\dfrac{\partial u_j}{\partial x} + \dfrac{\partial v_j}{\partial y}\right) + w_j\left(\dfrac{\partial h_j}{\partial x}\dfrac{\partial w_j}{\partial x} + \dfrac{\partial h_j}{\partial y}\dfrac{\partial w_j}{\partial y}\right) \end{array}\right] \\
+ \rho\frac{\left(z-h_j\right)^2}{2} & \left\{\begin{array}{l} \dfrac{\partial^2 u_j}{\partial t\partial x} + \dfrac{\partial^2 v_j}{\partial t\partial y} - \dfrac{\partial h_j}{\partial x}\dfrac{\partial^2 w_j}{\partial t\partial x} - \dfrac{\partial h_j}{\partial y}\dfrac{\partial^2 w_j}{\partial t\partial y} - \left(\dfrac{\partial w_j}{\partial x}\right)^2 - \left(\dfrac{\partial w_j}{\partial y}\right)^2 - \left(\dfrac{\partial u_j}{\partial x} + \dfrac{\partial v_j}{\partial y}\right)^2 \\ + u_j\left(\dfrac{\partial^2 u_j}{\partial x^2} + \dfrac{\partial^2 u_j}{\partial y^2}\right) + v_j\left(\dfrac{\partial^2 v_j}{\partial x^2} + \dfrac{\partial^2 v_j}{\partial y^2}\right) + w_j\left(\dfrac{\partial^2 w_j}{\partial x^2} + \dfrac{\partial^2 w_j}{\partial y^2}\right) \end{array}\right\} \\
& + O\left[\left(\frac{\partial h_j}{\partial x}\right)^2, \frac{\partial h_j}{\partial x}\frac{\partial h_j}{\partial y}, \left(\frac{\partial h_j}{\partial y}\right)^2, \frac{\partial^2 h_j}{\partial x\partial y}, \frac{\partial^2 h_j}{\partial x^2}, \frac{\partial^2 h_j}{\partial y^2}\right]
\end{aligned}
\tag{40}
$$

For the corresponding first-order derivatives,

$$
\begin{aligned}
\left(\frac{\partial q}{\partial x}\right)_j = \frac{\partial q_j}{\partial x} + \rho\frac{\partial h_j}{\partial x}\left[\frac{\partial w_j}{\partial t} + u_j\frac{\partial w_j}{\partial x} + v_j\frac{\partial w_j}{\partial y} - w_j\left(\frac{\partial u_j}{\partial x} + \frac{\partial v_j}{\partial y}\right)\right] \\
+ O\left[\left(\frac{\partial h_j}{\partial x}\right)^2, \frac{\partial h_j}{\partial x}\frac{\partial h_j}{\partial y}, \left(\frac{\partial h_j}{\partial y}\right)^2\right]
\end{aligned}
\tag{41}
$$

$$
\begin{aligned}
\left(\frac{\partial q}{\partial y}\right)_j = \frac{\partial q_j}{\partial y} + \rho\frac{\partial h_j}{\partial y}\left[\frac{\partial w_j}{\partial t} + u_j\frac{\partial w_j}{\partial x} + v_j\frac{\partial w_j}{\partial y} - w_j\left(\frac{\partial u_j}{\partial x} + \frac{\partial v_j}{\partial y}\right)\right] \\
+ O\left[\left(\frac{\partial h_j}{\partial x}\right)^2, \frac{\partial h_j}{\partial x}\frac{\partial h_j}{\partial y}, \left(\frac{\partial h_j}{\partial y}\right)^2\right]
\end{aligned}
\tag{42}
$$

In each layer, the horizontal momentum Eq. (1) may be written as

$$
\frac{\partial u_j}{\partial t} + u_j\left(\frac{\partial u}{\partial x}\right)_j + v_j\left(\frac{\partial u}{\partial y}\right)_j + w_j\left(\frac{\partial u}{\partial z}\right)_j = -g\frac{\partial \zeta}{\partial x} - \frac{1}{\rho}\left(\frac{\partial q}{\partial x}\right)_j
\tag{43}
$$

Incorporating the irrotationality condition in Eq. (6), Eq. (43) becomes

$$
\frac{\partial u_j}{\partial t} + u_j\left(\frac{\partial u}{\partial x}\right)_j + v_j\left(\frac{\partial u}{\partial y}\right)_j + w_j\left(\frac{\partial w}{\partial x}\right)_j = -g\frac{\partial \zeta}{\partial x} - \frac{1}{\rho}\left(\frac{\partial q}{\partial x}\right)_j
\tag{44}
$$

Combining with Eqs. (23), (24), (21) and (40), Eq. (44) can be now rewritten as

$$
\frac{\partial u_j}{\partial t} + u_j\frac{\partial u_j}{\partial x} + v_j\frac{\partial u_j}{\partial y} + w_j\frac{\partial w_j}{\partial x} = -g\frac{\partial \zeta}{\partial x} - \frac{1}{\rho}\frac{\partial q_j}{\partial x} + v_j\frac{\partial h_j}{\partial y}\frac{\partial w_j}{\partial y} - \frac{\partial h_j}{\partial x}\left(\frac{\partial w_j}{\partial t} + v_j\frac{\partial w_j}{\partial y}\right)
\tag{45}
$$

Similar expression can be obtained for the horizontal momentum Eq. (2), *i.e.*

$$
\frac{\partial v_j}{\partial t} + u_j\frac{\partial v_j}{\partial x} + v_j\frac{\partial v_j}{\partial y} + w_j\frac{\partial w_j}{\partial y} = -g\frac{\partial \zeta}{\partial y} - \frac{1}{\rho}\frac{\partial q_j}{\partial y} + u_j\frac{\partial h_j}{\partial x}\frac{\partial w_j}{\partial x} - \frac{\partial h_j}{\partial y}\left(\frac{\partial w_j}{\partial t} + u_j\frac{\partial w_j}{\partial x}\right)
\tag{46}
$$

With Eq. (40), the dynamic boundary condition in Eq. (7) can now be expressed as

$$
\begin{aligned}
q_N = {} & \rho\left(\zeta - h_N\right)\left[\begin{aligned} & \frac{\partial w_N}{\partial t} + u_N \frac{\partial w_N}{\partial x} + v_N \frac{\partial w_N}{\partial y} - w_N\left(\frac{\partial u_N}{\partial x} + \frac{\partial v_N}{\partial y}\right) \\ & + \left(u_N \frac{\partial h_N}{\partial x} + v_N \frac{\partial h_N}{\partial y}\right)\left(\frac{\partial u_N}{\partial x} + \frac{\partial v_N}{\partial y}\right) + w_N\left(\frac{\partial h_N}{\partial x}\frac{\partial w_N}{\partial x} + \frac{\partial h_N}{\partial y}\frac{\partial w_N}{\partial y}\right) \end{aligned}\right] \\
& - \rho \frac{\left(\zeta - h_N\right)^2}{2}\left\{\begin{aligned} & \frac{\partial^2 u_N}{\partial t \partial x} + \frac{\partial^2 v_N}{\partial t \partial y} - \left(\frac{\partial w_N}{\partial x}\right)^2 - \left(\frac{\partial w_N}{\partial y}\right)^2 - \left(\frac{\partial u_N}{\partial x} + \frac{\partial v_N}{\partial y}\right)^2 \\ & + u_N\left(\frac{\partial^2 u_N}{\partial x^2} + \frac{\partial^2 u_N}{\partial y^2}\right) + v_N\left(\frac{\partial^2 v_N}{\partial x^2} + \frac{\partial^2 v_N}{\partial y^2}\right) + w_N\left(\frac{\partial^2 w_N}{\partial x^2} + \frac{\partial^2 w_N}{\partial y^2}\right) \\ & - \frac{\partial h_N}{\partial x}\frac{\partial^2 w_N}{\partial t \partial x} - \frac{\partial h_N}{\partial y}\frac{\partial^2 w_N}{\partial t \partial y} \end{aligned}\right\}
\end{aligned} \tag{47}
$$

Combining equations (33)-(35), the kinematic boundary condition in Eq. (8) and the bottom boundary condition in Eq. (9) can be respectively rewritten as

$$
\begin{aligned}
w_N - \frac{\partial \zeta}{\partial t} - u_N \frac{\partial \zeta}{\partial x} - v_N \frac{\partial \zeta}{\partial y} = {} & \left(\zeta - h_N\right)\left(\frac{\partial u_N}{\partial x} + \frac{\partial v_N}{\partial y} + \frac{\partial \zeta}{\partial x}\frac{\partial w_N}{\partial x} + \frac{\partial \zeta}{\partial y}\frac{\partial w_N}{\partial y}\right) \\
& + \left(\zeta - h_N\right)\left[\left(\frac{\partial \zeta}{\partial x}\frac{\partial h_N}{\partial x} + \frac{\partial \zeta}{\partial y}\frac{\partial h_N}{\partial y}\right)\left(\frac{\partial u_N}{\partial x} + \frac{\partial v_N}{\partial y}\right) - \left(\frac{\partial h_N}{\partial x}\frac{\partial w_N}{\partial x} + \frac{\partial h_N}{\partial y}\frac{\partial w_N}{\partial y}\right)\right] \\
& + \frac{\left(\zeta - h_N\right)^2}{2}\left\{\frac{\partial^2 w_N}{\partial x^2} + \frac{\partial^2 w_N}{\partial y^2} - \left(\frac{\partial^2 u_N}{\partial x^2} + \frac{\partial^2 u_N}{\partial y^2}\right)\frac{\partial \zeta}{\partial x} - \left(\frac{\partial^2 v_N}{\partial x^2} + \frac{\partial^2 v_N}{\partial y^2}\right)\frac{\partial \zeta}{\partial y}\right\}
\end{aligned} \tag{48}
$$

and

$$
\begin{aligned}
w_1 + u_1 \frac{\partial d}{\partial x} + v_1 \frac{\partial d}{\partial y} = {} & \left(d + h_1\right)\left\{\begin{aligned} & \frac{\partial d}{\partial x}\frac{\partial w_1}{\partial x} + \frac{\partial d}{\partial y}\frac{\partial w_1}{\partial y} + \frac{\partial h_1}{\partial x}\left[\frac{\partial w_1}{\partial x} + \frac{\partial d}{\partial x}\left(\frac{\partial u_1}{\partial x} + \frac{\partial v_1}{\partial y}\right)\right] \\ & - \left(\frac{\partial u_1}{\partial x} + \frac{\partial v_1}{\partial y}\right) + \frac{\partial h_1}{\partial y}\left[\frac{\partial w_1}{\partial y} + \frac{\partial d}{\partial y}\left(\frac{\partial u_1}{\partial x} + \frac{\partial v_1}{\partial y}\right)\right] \end{aligned}\right\} \\
& + \frac{\left(d + h_1\right)^2}{2}\left[\frac{\partial d}{\partial x}\left(\frac{\partial^2 u_1}{\partial x^2} + \frac{\partial^2 u_1}{\partial y^2}\right) + \frac{\partial d}{\partial y}\left(\frac{\partial^2 v_1}{\partial x^2} + \frac{\partial^2 v_1}{\partial y^2}\right) + \left(\frac{\partial^2 w_1}{\partial x^2} + \frac{\partial^2 w_1}{\partial y^2}\right)\right]
\end{aligned} \tag{49}
$$

Assuming continuous velocities and pressure across an interface, the Taylor series expanded flow variables with respect to h_j at interface z_j must be equal to those based on h_{j+1}, *i.e.*

$$
u_{z_j}^{h_j} = u_{z_j}^{h_{j+1}} \qquad v_{z_j}^{h_j} = v_{z_j}^{h_{j+1}} \qquad w_{z_j}^{h_j} = w_{z_j}^{h_{j+1}} \qquad q_{z_j}^{h_j} = q_{z_j}^{h_{j+1}} \tag{50}
$$

The continuity equation Eq. (4) and the irrotationality condition Eq. (6) have been commonly used to derive the expressions for velocities u, v and w and the nonhydrostatic pressure q in each layer. Any two of the above four continuity relationships can be deduced by the other two. Taking the horizontal velocity u and the vertical velocity w as examples, using their expressions (33) and (35), the above continuity condition across the interface lead to

$$\begin{aligned} &u_j + \left(z_j - h_j\right)\left[\frac{\partial w_j}{\partial x} + \frac{\partial h_j}{\partial x}\left(\frac{\partial u_j}{\partial x} + \frac{\partial v_j}{\partial y}\right)\right] - \frac{\left(z - h_j\right)^2}{2}\left(\frac{\partial^2 u_j}{\partial x^2} + \frac{\partial^2 u_j}{\partial y^2}\right) = \\ &u_{j+1} + \left(z_j - h_{j+1}\right)\left[\frac{\partial w_{j+1}}{\partial x} + \frac{\partial h_{j+1}}{\partial x}\left(\frac{\partial u_{j+1}}{\partial x} + \frac{\partial v_{j+1}}{\partial y}\right)\right] - \frac{\left(z_j - h_{j+1}\right)^2}{2}\left(\frac{\partial^2 u_{j+1}}{\partial x^2} + \frac{\partial^2 u_{j+1}}{\partial y^2}\right) \end{aligned} \quad (51)$$

$$\begin{aligned} &w_j - \left(z_j - h_j\right)\left(\frac{\partial u_j}{\partial x} + \frac{\partial v_j}{\partial y} - \frac{\partial h_j}{\partial x}\frac{\partial w_j}{\partial x} - \frac{\partial h_j}{\partial y}\frac{\partial w_j}{\partial y}\right) - \frac{\left(z_j - h_j\right)^2}{2}\left(\frac{\partial^2 w_j}{\partial x^2} + \frac{\partial^2 w_j}{\partial y^2}\right) = \\ &w_{j+1} - \left(z_j - h_{j+1}\right)\left(\frac{\partial u_{j+1}}{\partial x} + \frac{\partial v_{j+1}}{\partial y} - \frac{\partial h_{j+1}}{\partial x}\frac{\partial w_{j+1}}{\partial x} - \frac{\partial h_{j+1}}{\partial y}\frac{\partial w_{j+1}}{\partial y}\right) - \frac{\left(z_j - h_{j+1}\right)^2}{2}\left(\frac{\partial^2 w_{j+1}}{\partial x^2} + \frac{\partial^2 w_{j+1}}{\partial y^2}\right) \end{aligned}$$

(52)

Whilst deriving the new multilayer equation system, all of the z-direction derivatives have been automatically eliminated, leading to a much-simplified formulation. Unlike Boussinesq-type equations, the vertical velocity w and pressure q are not expanded in the form of horizontal velocities u and v in order to prevent higher order derivative terms in the equations. In turn, these simplified equations can be numerically discretized using simpler numerical scheme, minimizing the possible numerical errors caused by sophisticated vertical discretization near to the bathymetry with abrupt changes.

RESULTS

As a summary, the multilayer nonhydrostatic momentum equations are given as follows

$$\frac{\partial u_j}{\partial t} + u_j\frac{\partial u_j}{\partial x} + v_j\frac{\partial u_j}{\partial y} + w_j\frac{\partial w_j}{\partial x} = -g\frac{\partial \zeta}{\partial x} - \frac{1}{\rho}\frac{\partial q_j}{\partial x} + v_j\frac{\partial h_j}{\partial y}\frac{\partial w_j}{\partial y} - \frac{\partial h_j}{\partial x}\left(\frac{\partial w_j}{\partial t} + v_j\frac{\partial w_j}{\partial y}\right) \quad (53)$$

$$\frac{\partial v_j}{\partial t} + u_j\frac{\partial v_j}{\partial x} + v_j\frac{\partial v_j}{\partial y} + w_j\frac{\partial w_j}{\partial y} = -g\frac{\partial \zeta}{\partial y} - \frac{1}{\rho}\frac{\partial q_j}{\partial y} + u_j\frac{\partial h_j}{\partial x}\frac{\partial w_j}{\partial x} - \frac{\partial h_j}{\partial y}\left(\frac{\partial w_j}{\partial t} + u_j\frac{\partial w_j}{\partial x}\right) \quad (54)$$

with the following free-surface boundary conditions

$$
q_N = \rho\left(\zeta - h_N\right)\left[\begin{array}{l} \dfrac{\partial w_N}{\partial t} + u_N \dfrac{\partial w_N}{\partial x} + v_N \dfrac{\partial w_N}{\partial y} - w_N\left(\dfrac{\partial u_N}{\partial x} + \dfrac{\partial v_N}{\partial y}\right) \\ + \left(u_N \dfrac{\partial h_N}{\partial x} + v_N \dfrac{\partial h_N}{\partial y}\right)\left(\dfrac{\partial u_N}{\partial x} + \dfrac{\partial v_N}{\partial y}\right) + w_N\left(\dfrac{\partial h_N}{\partial x}\dfrac{\partial w_N}{\partial x} + \dfrac{\partial h_N}{\partial y}\dfrac{\partial w_N}{\partial y}\right) \end{array}\right]
$$

$$
- \rho\frac{\left(\zeta - h_N\right)^2}{2}\left\{\begin{array}{l} \dfrac{\partial^2 u_N}{\partial t \partial x} + \dfrac{\partial^2 v_N}{\partial t \partial y} - \left(\dfrac{\partial w_N}{\partial x}\right)^2 - \left(\dfrac{\partial w_N}{\partial y}\right)^2 - \left(\dfrac{\partial u_N}{\partial x} + \dfrac{\partial v_N}{\partial y}\right)^2 \\ + u_N\left(\dfrac{\partial^2 u_N}{\partial x^2} + \dfrac{\partial^2 u_N}{\partial y^2}\right) + v_N\left(\dfrac{\partial^2 v_N}{\partial x^2} + \dfrac{\partial^2 v_N}{\partial y^2}\right) + w_N\left(\dfrac{\partial^2 w_N}{\partial x^2} + \dfrac{\partial^2 w_N}{\partial y^2}\right) \\ - \dfrac{\partial h_N}{\partial x}\dfrac{\partial^2 w_N}{\partial t \partial x} - \dfrac{\partial h_N}{\partial y}\dfrac{\partial^2 w_N}{\partial t \partial y} \end{array}\right\} \tag{55}
$$

$$
\begin{aligned}
w_N - \frac{\partial \zeta}{\partial t} - u_N \frac{\partial \zeta}{\partial x} - v_N \frac{\partial \zeta}{\partial y} &= \left(\zeta - h_N\right)\left(\frac{\partial u_N}{\partial x} + \frac{\partial v_N}{\partial y} + \frac{\partial \zeta}{\partial x}\frac{\partial w_N}{\partial x} + \frac{\partial \zeta}{\partial y}\frac{\partial w_N}{\partial y}\right) \\
&+ \left(\zeta - h_N\right)\left[\left(\frac{\partial \zeta}{\partial x}\frac{\partial h_N}{\partial x} + \frac{\partial \zeta}{\partial y}\frac{\partial h_N}{\partial y}\right)\left(\frac{\partial u_N}{\partial x} + \frac{\partial v_N}{\partial y}\right) - \left(\frac{\partial h_N}{\partial x}\frac{\partial w_N}{\partial x} + \frac{\partial h_N}{\partial y}\frac{\partial w_N}{\partial y}\right)\right] \\
&+ \frac{\left(\zeta - h_N\right)^2}{2}\left\{\frac{\partial^2 w_N}{\partial x^2} + \frac{\partial^2 w_N}{\partial y^2} - \left(\frac{\partial^2 u_N}{\partial x^2} + \frac{\partial^2 u_N}{\partial y^2}\right)\frac{\partial \zeta}{\partial x} - \left(\frac{\partial^2 v_N}{\partial x^2} + \frac{\partial^2 v_N}{\partial y^2}\right)\frac{\partial \zeta}{\partial y}\right\}
\end{aligned} \tag{56}
$$

the bottom boundary condition

$$
\begin{aligned}
w_1 + u_1 \frac{\partial d}{\partial x} + v_1 \frac{\partial d}{\partial y} &= \left(d + h_1\right)\left\{\begin{array}{l} \dfrac{\partial d}{\partial x}\dfrac{\partial w_1}{\partial x} + \dfrac{\partial d}{\partial y}\dfrac{\partial w_1}{\partial y} + \dfrac{\partial h_1}{\partial x}\left[\dfrac{\partial w_1}{\partial x} + \dfrac{\partial d}{\partial x}\left(\dfrac{\partial u_1}{\partial x} + \dfrac{\partial v_1}{\partial y}\right)\right] \\ - \left(\dfrac{\partial u_1}{\partial x} + \dfrac{\partial v_1}{\partial y}\right) + \dfrac{\partial h_1}{\partial y}\left[\dfrac{\partial w_1}{\partial y} + \dfrac{\partial d}{\partial y}\left(\dfrac{\partial u_1}{\partial x} + \dfrac{\partial v_1}{\partial y}\right)\right] \end{array}\right\} \\
&+ \frac{\left(d + h_1\right)^2}{2}\left[\frac{\partial d}{\partial x}\left(\frac{\partial^2 u_1}{\partial x^2} + \frac{\partial^2 u_1}{\partial y^2}\right) + \frac{\partial d}{\partial y}\left(\frac{\partial^2 v_1}{\partial x^2} + \frac{\partial^2 v_1}{\partial y^2}\right) + \left(\frac{\partial^2 w_1}{\partial x^2} + \frac{\partial^2 w_1}{\partial y^2}\right)\right]
\end{aligned} \tag{57}
$$

and the continuity conditions across an interface of layers (if more than one layers are used)

$$
\begin{aligned}
&u_j + \left(z_j - h_j\right)\left[\frac{\partial w_j}{\partial x} + \frac{\partial h_j}{\partial x}\left(\frac{\partial u_j}{\partial x} + \frac{\partial v_j}{\partial y}\right)\right] - \frac{\left(z - h_j\right)^2}{2}\left(\frac{\partial^2 u_j}{\partial x^2} + \frac{\partial^2 u_j}{\partial y^2}\right) = \\
&u_{j+1} + \left(z_j - h_{j+1}\right)\left[\frac{\partial w_{j+1}}{\partial x} + \frac{\partial h_{j+1}}{\partial x}\left(\frac{\partial u_{j+1}}{\partial x} + \frac{\partial v_{j+1}}{\partial y}\right)\right] - \frac{\left(z_j - h_{j+1}\right)^2}{2}\left(\frac{\partial^2 u_{j+1}}{\partial x^2} + \frac{\partial^2 u_{j+1}}{\partial y^2}\right)
\end{aligned} \tag{58}
$$

$$
\begin{aligned}
&w_j - \left(z_j - h_j\right)\left(\frac{\partial u_j}{\partial x} + \frac{\partial v_j}{\partial y} - \frac{\partial h_j}{\partial x}\frac{\partial w_j}{\partial x} - \frac{\partial h_j}{\partial y}\frac{\partial w_j}{\partial y}\right) - \frac{\left(z_j - h_j\right)^2}{2}\left(\frac{\partial^2 w_j}{\partial x^2} + \frac{\partial^2 w_j}{\partial y^2}\right) = \\
&w_{j+1} - \left(z_j - h_{j+1}\right)\left(\frac{\partial u_{j+1}}{\partial x} + \frac{\partial v_{j+1}}{\partial y} - \frac{\partial h_{j+1}}{\partial x}\frac{\partial w_{j+1}}{\partial x} - \frac{\partial h_{j+1}}{\partial y}\frac{\partial w_{j+1}}{\partial y}\right) - \frac{\left(z_j - h_{j+1}\right)^2}{2}\left(\frac{\partial^2 w_{j+1}}{\partial x^2} + \frac{\partial^2 w_{j+1}}{\partial y^2}\right)
\end{aligned}
$$

(59)

The above N-layer nonhydrostatic equation system consists of $2N$ momentum equations, three sets of boundary conditions and $2(N-1)$ continuity conditions, a total of $4N+1$ coupled equations for $4N+1$ variables including u_j, v_j, w_j and q_j ($j = 1 \sim N$) and an additional free surface elevation ζ.

The above governing equations only possess derivatives of up to second-order, which can be easily and efficiently solved using a well-established numerical method, *e.g.* finite difference method, finite volume method and finite element method. For numerical implementation, the system of equations may be solved in two steps: hydrostatic step and nonhydrostatic step. The hydrostatic components (*i.e.* the governing equations without considering the nonhydrostatic pressure effect) are solved in the hydrostatic step while the nonhydrostatic pressure terms are computed in the second step. In the nonhydrostatic step, the relationships between u_j, v_j, w_j and q_j are given in Eqs.(53)-(55), which are substituted into the bottom condition Eq.(57) to give an elliptic equation for the non-hydrostatic pressure. The focus of this work is to introduce the new multilayer nonhydrostatic formulation for surface water waves. The corresponding numerical model is currently being developed and will be presented in a future paper.

Although the above governing equations are derived for gravity water waves, it has not predefined any specific vertical profiles for the velocities and pressure and therefore they can indeed provide more natural vertical profiles for these variables, as shown in the theoretical analysis in the following section.

ANALYSIS

The new multilayer governing equations should be further analyzed to reveal their properties and optimize parameterization. The analyses undertaken herein are limited to one horizontal dimension for simplicity, but the procedure and conclusions can be directly extended to the two-dimension case. The optimized values for coefficients α_j and β_j will be obtained by analyzing the linear properties of the equations, including the linear dispersion, linear shoaling and linear velocity profile. The nonlinear properties of the formulations are further examined after these coefficients are determined.

Fourier Analysis

Stoke-type Fourier analysis is conducted to obtain the linear and nonlinear second and third harmonics of the governing equations (Madsen, Bingham and Liu, 2002). The first-, second- and third-order solutions may be extracted through a perturbation expansion

$$\zeta = \varepsilon A^{(1)} \cos(kx-\omega t) + \varepsilon^2 A^{(2)} \cos 2(kx-\omega t) + \varepsilon^3 A^{(3)} \cos 3(kx-\omega t) \quad (60)$$

$$u_j = \varepsilon U_j^{(1)} \cos(kx-\omega t) + \varepsilon^2 U_j^{(2)} \cos 2(kx-\omega t) + \varepsilon^3 U_j^{(3)} \cos 3(kx-\omega t) \quad (61)$$

$$w_j = -\varepsilon W_j^{(1)} \sin(kx-\omega t) - \varepsilon^2 W_j^{(2)} \sin 2(kx-\omega t) - \varepsilon^3 W_j^{(3)} \sin 3(kx-\omega t) \quad (62)$$

$$q_j = \varepsilon Q_j^{(1)} \cos(kx-\omega t) + \varepsilon^2 Q_j^{(2)} \cos 2(kx-\omega t) + \varepsilon^3 Q_j^{(3)} \cos 3(kx-\omega t) \quad (63)$$

where ε is a small perturbation parameter, $A^{(i)}$, $U_j^{(i)}$, $W_j^{(i)}$ and $Q_j^{(i)}$ are real functions (i = 1, 2 and 3), k is the wavenumber, and ω is the cyclic frequency. To avoid unbounded solutions at the third order, the frequency and first-order solutions are expanded as follows

$$\omega = \omega\left(1+\varepsilon^2\omega^{(13)}\right),\ U_j^{(1)} = U_j^{(1)}\left(1+\varepsilon^2 U_j^{(13)}\right),\ W_j^{(1)} = W_j^{(1)}\left(1+\varepsilon^2 W_j^{(13)}\right),\ Q_j^{(1)} = Q_j^{(1)}\left(1+\varepsilon^2 Q_j^{(13)}\right)$$

(64)

where superscript (13) denotes the third-order terms arisen from the first-order solutions. Substituting Eq. (60) - (64) into the governing equations Eq. (53), (55)-(59) and collating all the terms of order $O(\varepsilon^n)$ will lead to the first, second and third-order solutions. Results from the analysis for the first-three-layer formulations are compared with the exact Stokes solutions (Fenton, 1985; Kennedy *et al.*, 2001).

Shoaling Analysis

In one horizontal dimension with a slowly varying bathymetry $d = d(\varepsilon x)$, solutions of the following form may be sought by following Madsen, Bingham and Liu (2002),

$$\zeta = A^{(1)}\exp\left\{\mathrm{i}\left[\omega t-\int k(x)\,\mathrm{d}x\right]\right\},\qquad u_j = U_j^{(1)}\left(1+\mathrm{i}\sigma_j^1 d_x\right)\exp\left\{\mathrm{i}\left[\omega t-\int k(x)\,\mathrm{d}x\right]\right\}$$
$$w_j = \mathrm{i}W_j^{(1)}\left(1+\mathrm{i}\sigma_j^2 d_x\right)\exp\left\{\mathrm{i}\left[\omega t-\int k(x)\,\mathrm{d}x\right]\right\},\qquad q_j = Q_j^{(1)}\left(1+\mathrm{i}\sigma_j^3 d_x\right)\exp\left\{\mathrm{i}\left[\omega t-\int k(x)\,\mathrm{d}x\right]\right\}$$

(65)

where i is the imaginary unit, σ_j^i is introduced to account for a small phase due to a slowly varying bottom. Substituting Eq. (65) into the linearized formulation and keeping only the first-order derivatives, it obtains the real and imaginary parts of the solutions. $U_j^{(1)}$, $W_j^{(1)}$ and $Q_j^{(1)}$ are solved in terms of $A^{(1)}$ to give the first-order solutions for monochromatic waves on a slowly varying bottom. Further eliminating σ_j^i, $U_{jx}^{(1)}$, $W_{jx}^{(1)}$ and $Q_{jx}^{(1)}$ yields the equation in the form of

$$\frac{A_x}{A} = -s_0\frac{dx}{d} \tag{66}$$

where s_0 is the shoaling coefficient. The equation will be analyzed by comparing with the shoaling gradient from Stokes linear theory (Madsen and Sørensen, 1992).

DISCUSSION

Stoke-type Fourier and shoaling analyses are carried out to scrutinize the mathematical properties of the new formulation. The representative interface and the location to define variables in each layer are optimized to improve model accuracy.

One-Layer Formulation

The one-layer formulation involves four variables, *i.e.* ζ, u_1, w_1, q_1, which can be obtained by solving Eq. (53), (55), (56) and (57). The specific expressions for the first-, second- and third-order solutions for monochromatic waves on a horizontal bottom and the shoaling coefficient can be obtained using Wolfram Mathematica. The corresponding dispersion relation, the associated velocities and the shoaling coefficient are detailed in Appendix A.

Through examination of linear property, the most accurate set of the representative interface and the location to define variables will be chosen. The coefficient β_1 can be directly determined by fitting the calculated phase speed c or the group velocity c_g with the exact linear solution for Stokes waves. However, as the velocity profile may play an important role in wave-structure interaction and the shoaling coefficient is a fundamental quantity for wave propagation over varying bathymetry, optimized value of β_1 is obtained by minimizing the errors for phase speed, group velocity, shoaling effect and velocity profiles following the method of Lynett and Liu (2004a), *i.e.*

$$\Delta_{\text{linear}}=\frac{1}{5}\left(\sum_{kd=0.1}^{\Omega}\left|\frac{c^{\mathrm{e}}-c}{c^{\mathrm{e}}}\right|+\sum_{kd=0.1}^{\Omega}\left|\frac{c_{\mathrm{g}}^{\mathrm{e}}-c_{g}}{c_{\mathrm{g}}^{\mathrm{e}}}\right|+\sum_{kd=0.1}^{\Omega}\left|\frac{s_0^{\mathrm{e}}-s_0}{s_0^{\mathrm{e}}}\right|+\sum_{kd=0.1}^{\Omega}\left|\frac{\int_{-d}^{0}\left[u^{\mathrm{e}}(z)-u(z)\right]dz}{\int_{-d}^{0}u^{\mathrm{e}}(z)dz}\right|+\sum_{kd=0.1}^{\Omega}\left|\frac{\int_{-d}^{0}\left[w^{\mathrm{e}}(z)-w(z)\right]dz}{\int_{-d}^{0}w^{\mathrm{e}}(z)dz}\right|\right) \tag{67}$$

where the superscript e denotes the exact solution from the Stokes theory. As the one-layer model is supposed to be applied in coastal wave transformation that generally occurs when water depth *kd* is less than π, β_1 is thus optimized over the range $\Omega = \pi$, leading to $\beta_1 = 0.50$ and $\Delta_{\text{linear}} = 0.014$.

The resulting phase speed, wave group celerity and shoaling coefficient for the one-layer model are plotted in Figure 2. The model has a maximum error of less than 3% for the phase speed and less than 10% for the group velocity in the entire range, which has the similar accuracy as the second-order dispersion Boussinesq equations derived by Nwogu (1993) and Madsen, Murray and Sørensen (1991). The shoaling coefficient has an excellent agreement with the Stokes first theory for $\Omega \leq 5/8\pi$. However, the discrepancy increases monotonically with *kd* beyond this range.

The vertical profiles of horizontal and vertical velocities are plotted in Figure 3, showing good agreement with those resulting from the linear Stokes theory, especially for the vertical velocity component. The predicted horizontal velocity near to the bottom is slightly larger than that from the Stokes theory, especially for high wavenumbers. The possible reason may be that the water motion is predominantly horizontal and vertical velocity is much weaker than the horizontal velocity in shallow and intermediate water. The solutions from one-layer model agree more favorably with the exact solutions than the second-order Boussinesq theory as reported by Gobbi, Kirby and Wei (2000). The reason may lie in the fact that the current formulation does not predefine the vertical velocity structures as the Boussinesq theories do.

Following the procedure of solving the Stokes water theory, the first-order solutions provide forcing to drive the second-order solutions; the first and second-order solutions together provide forcing to the third-order solutions. The corresponding second- and third-order solutions are provided in Appendix A.

Stokes wave theory gives the second- and third-harmonic amplitudes

$$a_{\text{Stokes}}^{(2)} = \frac{ka^{(1)2}}{4} \frac{\cosh kd \left(2\cosh^2 kd + 1\right)}{\sinh^3 kd} \tag{68}$$

and

$$a_{\text{Stokes}}^{(3)} = \frac{3k^2 a^{(1)3}}{64} \frac{8\cosh^6 kd + 1}{\sinh^6 kd} \tag{69}$$

They are used as references for comparison with the solutions obtained from the present formulations.

Figure 4 compares the second- and third-order wave amplitudes from the one-layer model and Boussinesq equations of Nwogu (1993). As the results are normalized with Stokes solutions (68) and (69), the unity indicates perfect agreement. The Boussinesq solutions converge to the Stokes solution as kd approaches zero. The one-layer system exhibits different convergence patterns, and there are offsets towards $kd = 0$ for the second- and third-order solutions. The similar results also appear at the multi-layer nonhydrostatic free-surface model from Bai and Cheung (2013), and they thought that it is due to the slower convergence of the dispersion relation in shallow water. As the present formulations have the similar accuracy as Boussinesq equations derived by Nwogu (1993) (see Figure 2), it prefers that these different convergence patterns might be due to the fact that Boussinesq equations usually express the vertical velocity w with one lower order polynomials than that for the horizontal velocities u and v while the present formulations describe them with the same order polynomials. Furthermore, Nwogu (1993) assumed the vertical velocity linearly varying and the horizontal velocities quadratically varying in the vertical direction respectively, however, this paper expresses all of them as quadratic polynomials. Such different kinematic structures may be the reason why distinct convergence characteristics are exhibited from Boussinesq equations and the present formulations. However, it must be emphasized that the solution from the one-layer system presents overall good agreement with the Stokes nonlinear theory for $kd \leq \pi$ than that from Nwogu (1993); the discrepancy for both the second and third-order solutions becomes less noticeable for larger kd.

Two-Layer Formulation

Considering the two-layer equation system in one horizontal dimension with a horizontal bottom, the dispersion relationship and velocities can be derived, which are listed in Appendix B with the corresponding shoaling coefficient.

The values of coefficients β_j and α_j can be again obtained by minimizing the error Δ_{linear} in Eq. (67) as for the one-layer system, *i.e.* $\Delta_{\text{linear}} = 0.014$. This yields $\Omega = 4\pi$, $\beta_1 = 0.641$, $\alpha_1 = 0.391$ and $\beta_2 = 0.305$, which are referred to as optimized coefficients herein. Most of the previous studies related to the optimization of coefficients for the Boussinesq-type equations considered only the shoaling effect and dispersion related characteristics, but neglected the vertical velocity structures (Gobbi, Kirby and Wei, 2000; Madsen, Murray and Sørensen, 1991; Nwogu, 1993; Schäffer and Madsen, 1995). Following these approaches (*i.e.* without considering the vertical velocity structures), coefficients are obtained and given by $\beta_1 = 0.895$, $\alpha_1 = 0.535$ and $\beta_2 = 0.105$, which are referred to as partially optimized coefficients.

Many numerical models based on the Navier-Stokes equations or the Euler equations adopt uniform layers in the vertical direction (Casulli and Stelling, 1998; Lin and Liu, 1998; Stelling and Zijlema, 2003; Zijlema and Stelling, 2005), except the model with non-uniform layers reported by Yuan and Wu (2006) that can achieve the same accuracy with less layers. Herein, the performance of the current formulation with uniform vertical layers is also examined. The associated coefficients for the current two-layer equation system are $\beta_1 = 0.75$, $\alpha_1 = 0.50$ and $\beta_2 = 0.25$, which are referred to as uniform-layer coefficients.

Figure 5 plots the phase speed, group velocity and shoaling effect with the three groups of coefficients as mentioned above. The coefficients obtained from Eq. (67) give the maximum errors of 1.0% and 4.5% for the phase speed and the group velocity respectively; the error corresponding to the shoaling coefficient increases as the wavenumber kd increases and reaches its maximum value (less than 0.06) at $kd = 4\pi$. It appears that the optimized coefficients obtained by neglecting vertical velocity structures provide the most accurate solutions for the phase speed, group velocity and shoaling effect, with relative errors less than 0.6% and 1.8% respectively for the phase speed and group velocity and absolute error less than 0.04 for the shoaling effect. For the model with uniform layers, the predicted phase speed is found to be closest to the exact solution; however, the errors for the group velocity and shoaling effect are the largest among the three sets of coefficients.

Figure 6 shows the horizontal and vertical velocities predicted by the two-layer equation system with aforementioned three groups of coefficients, in comparison with the exact linear solution for various relative water depth kd. The coefficients obtained from Eq. (67) lead to the most accurate results compared with the exact solution, even for $kd = 4\pi$. The model with two uniform layers also well represents the vertical velocity profiles, despite the slight deviation observed at the interface between the layers in the region with relative large water depth. Completely wrong velocity profiles are predicted for large kd with the partially optimized coefficients, which are obtained by only considering the phase speed, group velocity and shoaling effect. Both of the horizontal and vertical velocities should theoretically reach their maximum values at the free surface; however, the predicted vertical velocity profile with the partially optimized coefficients reaches its maximum at the interface between the two vertical layers; the medium-depth velocity is several times larger than that at the surface. Although these coefficients may lead to more accurate phase speed, group velocity and shoaling effect, they produce unacceptable velocity profiles and therefore will be discarded in the rest of this study. From now on, the two-layer equation system adopts $\beta_1 = 0.641$, $\alpha_1 = 0.391$, $\beta_2 = 0.305$ as the default optimized coefficients based on its overall good dispersion properties.

The two-layer equation system with the optimized coefficients provides much improved linear dispersion properties than the fourth-order Boussinesq equations derived by Gobbi, Kirby and Wei (2000). Their model gives a (4, 4) Padé dispersion relationship and the phase speed up to the range of $kd \approx 7$ with an error of 1% and the group velocity up to the range of $kd \approx 5$ with an error of 5%. Furthermore, the deviation between the Boussinesq model predicted vertical velocity profile and the exact linear theory becomes evidently when $kd \geq 8$. The present two-layer equation system with optimized coefficients also outshines the two-layer Boussinesq model derived by Lynett and Liu (2004a). Lynett and Liu's Boussinesq model can only predicts phase speed up to the range of $kd \approx 10$ and group velocity up to the range of $kd \approx 8$ with the same errors as the present two-layer model; the shoaling effect predicted by the present two-layer model has an overall much better accuracy. Additionally, the present two-layer equation system predicts a smooth vertical profile to a much higher degree of accuracy in a wider range; on the other hand, the Boussinesq model predicts a discontinuous vertical velocity gradient, causing an unphysical sharp change in the vertical velocity profile.

The second and third-order solutions for the two-layer equation system can be obtained using Mathematica, in a similar way as that for the one-layer formulations and are omitted here for simplicity. Figure 7 shows these solutions obtained using respectively the uniform-layer and default optimized coefficients, in comparison with the Stokes theory. The two second-order solutions are approximately anti-symmetry for $kd \leq 7\pi/4$. It is just coincidental and there is no specific physical reason behind it. Although the two-layer solutions with the optimized coefficients leads to slight larger error than the uniform-layer solutions in the special range $\pi/4 \leq kd \leq 7\pi/4$, they have an overall higher degree of accuracy over the optimized range $0 < kd \leq 4\pi$. The model with two uniform layers gives in a maximum error of 8% for the second-order solution and 14% for the third-order solution, while the model with optimized coefficients predicts a maximum error of 4% for the second-order solution and less than 9% for the third-order solution.

Three-Layer Formulation

The linear solutions including the dispersion relationship, phase speed, group velocity, shoaling coefficient and velocity profiles, as well as the second and third-order nonlinear solutions, to the three-layer model can be obtained in the same way as that for the one and two-layer formulations. All of the mathematical expressions are omitted here for simplicity and only results (comparison with analytical solutions) are discussed here.

Coefficients representing the phase speed, group velocity and shoaling effect obtained by following Eq. (67) are found to induce the same errors as the one and two-layer systems, *i.e.* $\Delta_{\text{linear}} = 0.014$, resulting in $\beta_1 = 0.965$, $\alpha_1 = 0.880$, $\beta_2 = 0.555$, $\alpha_2 = 0.185$, $\beta_3 = 0.118$ and the range of $\Omega = 10\pi$ (referred to as optimized coefficients). Figure 8 shows the resulting phase speed, group velocity and shoaling effect with these coefficients. The model with the optimized coefficients exhibits more accurate solutions, predicting a maximum relative error of 0.6% for the phase speed and of 1.2% for group velocity, compared with the 1.2% and 11.4% resulting from the uniform-layer model associated with the uniform-layer coefficients of $\beta_1 = 0.833$, $\alpha_1 = 0.667$, $\beta_2 = 0.500$, $\alpha_2 = 0.333$ and $\beta_3 = 0.167$. For the shoaling effect, the maximum absolute errors predicted by the two models are 0.025 and 0.271, respectively. The three-layer model with optimized coefficients is also superior to the four-layer Boussinesq model derived by Lynett and Liu (2004b) which gives maximum errors of more than 1% and 11% for phase speed and group velocity over the range $kd \leq 10\pi$. Furthermore, the three-layer model with optimized coefficients performs consistently better than the one and two-layer models within its application range.

Figure 9 presents the velocity profiles from the three-layer model with the optimized coefficients and the three-uniform-layer model. Large errors are observed on the vertical velocity profiles for both u and w from the three-uniform-layer model when $kd \geq 4\pi$ and the largest discrepancies are detected at the interfaces. On the other hand, the three-layer model with optimized coefficients predicts the vertical velocity profiles to a much higher degree of accuracy. Furthermore, the model is able to provides satisfactory results in extremely deep water, *e.g.* up to $kd = 10\pi$. The model is also superior than the four-layer Boussinesq model derived by Lynett and Liu (2004b) in predicting the vertical velocity profile which shows evident errors for $kd > 8\pi$.

Figure 10 presents the second- and third-order solutions to uniform-layer model and the model with optimized coefficients, in comparison with the analytical solution from the Stokes theory. The errors of the second and third-order solutions to the three-uniform-layer model increase as the kd increases and reach the maximum values of over 8% and 15% at $kd = 10\pi$. The model with optimized coefficients provides overall satisfactory second and third-order solutions, except for the range of $kd < 2\pi$. Considering the fact that the three-layer model is usually used in intermediate to deep water (outside the range of $kd < 2\pi$), the three-layer model with optimized coefficients can lead to reasonable accurate results.

CONCLUSIONS

A new formulation of the multilayer nonhydrostatic equations for surface water waves has been derived. The model defines velocities and pressure at an arbitrary location of a layer; subsequently the Taylor expansion is applied to derive the vertical flow field, and finally matches with the continuity conditions across the interface between two adjacent layers. With the maximum second-order spatial derivatives and identical structure of the formulations at different layers, the new governing equations can be numerically solved using a standard numerical scheme. Stoke-type Fourier and shoaling analyses have been carried out to scrutinize the properties of the new equations;

the representative interface and the unknowns evaluation locations in each layer are chosen to improve the model accuracy.

Optimization of the model coefficients for one-layer model is obtained for applications in the range of $kd \leq \pi$. The model with the optimized coefficients captures similar accurate linear and nonlinear wave behaviors to the existing second-order Boussinesq-type models (Madsen, Murray and Sørensen, 1991; Nwogu, 1993; Wei *et al.*, 1995). Optimized coefficients are derived for the two-layer model for applications in the range of $kd \leq 4\pi$. The resulting model predicts the phase speed and group velocity within the error bound of 1.0% and 4.5% and provides the second and third-order solutions within the error bound of 4% and 9%. It maintains better linear and nonlinear accuracy and has larger application range than existing four-order Boussinesq model and the two-layer Boussinesq model (Gobbi, Kirby and Wei, 2000; Lynett and Liu, 2004a). The linear and nonlinear optimization of the interface and variable evaluation locations for the three-layer model is implemented for the application range of $kd \leq 10\pi$. The model with the optimized coefficients exhibits accurate linearity for phase speed and group velocity within the error bound of 0.6% and 1.2% respectively, which effectively removes any shallow water limitation. It gives accurate nonlinear results towards the deep water for the second and third-order solutions within 2% and 4% of error bounds respectively, despite relatively large errors in the shallow-water region. Furthermore, as the current multilayer nonhydrostatic water wave model does not predefine the flow structures in the vertical direction and the optimization of coefficients considers the error in velocity profiles, it provides more accurate vertical profiles of the velocity field.

ACKNOWLEDGMENTS

This research was supported by National Key R&D Program of China (2017YFC1404205), National Natural Science Foundation of China (NSFC) (Grant No. 51579090) and the UK Royal Society and NSFC cost share International Exchanges award (Royal Society Ref. IE131297; NSFC Ref. 51411130125).

LITERATURE CITED

Agnon, Y.; Madsen, P.A., and Schaffer, H.A., 1999. A new approach to high-order Boussinesq models. *Journal of Fluid Mechanics*, 399, 319-333. 10.1017/s0022112099006394.

Ahmadi, A.; Badiei, P., and Namin, M.M., 2007. An implicit two-dimensional non-hydrostatic model for free-surface flows. *International Journal for Numerical Methods in Fluids*, 54(9), 1055-1074. 10.1002/fld.1414.

Bai, Y. and Cheung, K.F., 2013. Dispersion and nonlinearity of multi-layer non-hydrostatic free-surface flow. *Journal of Fluid Mechanics*, 726, 226-260. http://dx.doi.org/10.1017/jfm.2013.213.

Brocchini, M., 2013. A reasoned overview on Boussinesq-type models: the interplay between physics, mathematics and numerics. *Proceedings of the Royal Society A: Mathematical, Physical and Engineering Science*, 469(2160). 10.1098/rspa.2013.0496.

Casulli, V. and Stelling, G.S., 1998. Numerical simulation of 3D quasi-hydrostatic, free-surface flows. *Journal of Hydraulic Engineering-ASCE*, 124(7), 678-686. http://dx.doi.org/10.1061/(ASCE)0733-9429(1998)124:7(678).

Choi, D.Y.; Wu, C.H., and Young, C.-C., 2011. An efficient curvilinear non-hydrostatic model for simulating surface water waves. *International Journal for Numerical Methods in Fluids*, 66(9), 1093-1115. 10.1002/fld.2302.

Fenton, J.D., 1985. A Fifth‐Order Stokes Theory for Steady Waves. *Journal of Waterway, Port, Coastal and Ocean Engineering*, 111(C), 216-234. http://dx.doi.org/10.1061/(ASCE)0733-950X(1985)111:2(216).

Gobbi, M.F.; Kirby, J.T., and Wei, G., 2000. A fully nonlinear Boussinesq model for surface waves. Part 2. Extension to $O(kh)^{(4)}$. *Journal of Fluid Mechanics*, 405, 181-210. 10.1017/S0022112099007247.

Hirt, C.W. and Nichols, B.D., 1981. Volume of fluid (VOF) method for the dynamics of free boundaries. *Journal of Computational Physics*, 39(1), 201-225. http://dx.doi.org/10.1016/0021-9991(81)90145-5.

Kennedy, A.B.; Kirby, J.T.; Chen, Q., and Dalrymple, R.A., 2001. Boussinesq-type equations with improved nonlinear performance. *Wave Motion*, 33(3), 225-243. http://dx.doi.org/10.1016/S0165-2125(00)00071-8.

Lin, P.Z. and Liu, P.L.F., 1998. A numerical study of breaking waves in the surf zone. *Journal of Fluid Mechanics*, 359, 239-264. http://dx.doi.org/10.1017/S002211209700846X.

Liu, Z. and Fang, K., 2015. Two-layer Boussinesq models for coastal water waves. *Wave Motion*, 57(0), 88-111. http://dx.doi.org/10.1016/j.wavemoti.2015.03.006.

Lynett, P. and Liu, P.L.F., 2004a. A two-layer approach to wave modelling. *Proceedings of the Royal Society of London Series a-Mathematical Physical and Engineering Sciences*, 460(2049), 2637-2669. 10.1098/rspa.2004.1305.

Lynett, P. and Liu, P.L.F., 2004b. Linear analysis of the multi-layer model. *Coastal Engineering*, 51(5-6), 439–454. 10.1098/rspa.2004.1305.

Madsen, P.A. and Sørensen, O.R., 1992. A new form of the Boussinesq equations with improved linear dispersion characteristics. Part 2. A slowly-varying bathymetry. *Coastal Engineering*, 18(3–4), 183-204. 10.1016/0378-3839(92)90019-Q.

Madsen, P.A. and Schaffer, H.A., 1998. Higher-order Boussinesq-type equations for surface gravity waves: derivation and analysis. *Philosophical Transactions of the Royal Society of London Series a-Mathematical Physical and Engineering Sciences*, 356(1749), 3123-3184. 10.1098/rsta.1998.0309

Madsen, P.A.; Murray, R., and Sørensen, O.R., 1991. A new form of the Boussinesq equations with improved linear dispersion characteristics. *Coastal Engineering*, 15(4), 371-388. 10.1016/0378-3839(91)90017-B.

Madsen, P.A.; Bingham, H.B., and Liu, H., 2002. A new Boussinesq method for fully nonlinear waves from shallow to deep water. *Journal of Fluid Mechanics*, 462, 1-30. 10.1017/s0022112022008467.

Madsen, P.A.; Bingham, H.B., and Schaffer, H.A., 2003. Boussinesq-type formulations for fully nonlinear and extremely dispersive water waves: derivation and analysis. *Proceedings of the Royal Society of London Series a-Mathematical Physical and Engineering Sciences*, 459(2033), 1075-1104. 10.1098/rspa.2002.1067.

Nwogu, O., 1993. Alternative form of Boussinesq equations for nearshore wave propagation. *Journal of Waterway, Port, Coastal and Ocean Engineering*, 119(6), 618-638. 10.1061/(ASCE)0733-950X(1993)119:6(618).

Osher, S. and Fedkiw, R.P., 2001. Level Set Methods: An Overview and Some Recent Results. *Journal of Computational Physics*, 169(2), 463-502. http://dx.doi.org/10.1006/jcph.2000.6636.

Peregrine, D.H., 1967. Long waves on a beach. *Journal Fluid Mechanic*, 27(7), 815-827. 10.1017/S0022112067002605.

Schäffer, H.A. and Madsen, P.A., 1995. Further enhancements of Boussinesq-type equations. *Coastal Engineering*, 26(1-2), 1-14. 10.1016/0378-3839(95)00017-2.

Silva Santos, C.M.P. and Greaves, D.M., 2007. A mixed Lagrangian–Eulerian method for non-linear free surface flows using multigrid on hierarchical Cartesian grids. *Computers & Fluids*, 36(5), 914-923. http://dx.doi.org/10.1016/j.compfluid.2006.08.004.

Stelling, G. and Zijlema, M., 2003. An accurate and efficient finite-difference algorithm for non-hydrostatic free-surface flow with application to wave propagation. *International Journal for Numerical Methods in Fluids*, 43(1), 1-23. 10.1002/fld.595.

Wei, G.; Kirby, J.T.; Grilli, S.T., and Subramanya, R., 1995. A Fully Nonlinear Boussinesq Model for Surface-Waves .1. Highly Nonlinear Unsteady Waves. *Journal of Fluid Mechanics*, 294, 71-92. http://dx.doi.org/10.1017/S0022112095002813.

Young, C.C. and Wu, C.H., 2009. An efficient and accurate non-hydrostatic model with embedded Boussinesq-type like equations for surface wave modeling. *International Journal for Numerical Methods in Fluids*, 60(1), 27-53. 10.1002/fld.1876.

Yuan, H. and Wu, C.H., 2004. An implicit three-dimensional fully non-hydrostatic model for free-surface flows. *International Journal for Numerical Methods in Fluids*, 46(7), 709-733. 10.1002/fld.778.

Yuan, H. and Wu, C., 2006. Fully Nonhydrostatic Modeling of Surface Waves. *Journal of Engineering Mechanics*, 132(4), 447-456. doi:10.1061/(ASCE)0733-9399(2006)132:4(447).

Zhu, L.; Chen, Q., and Wan, X., 2014. Optimization of non-hydrostatic Euler model for water waves. *Coastal Engineering*, 91(0), 191-199. http://dx.doi.org/10.1016/j.coastaleng.2014.06.003.

Zijlema, M. and Stelling, G.S., 2005. Further experiences with computing non-hydrostatic free-surface flows involving water waves. *International Journal for Numerical Methods in Fluids*, 48(2), 169-197. 10.1002/fld.821.

APPENDIX A.

The corresponding dispersion relation for one-layer formulations is

$$\omega^2 = gk\frac{4kd + 2(1-\beta_1)\beta_1 k^3 d^3}{4 + 2d^2k^2 + (-1+\beta_1)^2\beta_1^2 d^4 k^4} \quad \text{(A.1)}$$

The associated velocities are

$$U^{(1)} = \frac{2gkA_1}{\omega}\frac{2 + k^2d^2(1-\beta_1)^2}{4 + 2k^2d^2 + (1-\beta_1)^2\beta_1^2 k^4 d^4} \quad \text{(A.2)}$$

and

$$W^{(1)} = -\frac{4(1-\beta_1)gdk^2A_1}{\omega\left[4 + 2d^2k^2 + (1-\beta_1)^2\beta_1^2 d^4 k^4\right]} \quad \text{(A.3)}$$

The shoaling coefficient for the one-layer formulation is

$$s = \frac{S_{10}^{(1)} + S_{12}^{(1)}k^2d^2 + S_{14}^{(1)}k^4d^4 + S_{16}^{(1)}k^6d^6 + S_{18}^{(1)}k^8d^8 + \mathrm{O}\left(k^{10}d^{10}\right)}{S_{20}^{(1)} + S_{22}^{(1)}k^2d^2 + S_{24}^{(1)}k^4d^4 + S_{26}^{(1)}k^6d^6 + S_{28}^{(1)}k^8d^8} \quad \text{(A.4)}$$

where

$$S_{10}^{(1)} = 4 \quad \text{(A.5)}$$

$$S_{12}^{(1)} = -6 + 14\beta_1 - 14\beta_1^2 \quad \text{(A.6)}$$

$$S_{14}^{(1)} = -6\beta_1^2 + 12\beta_1^3 - 6\beta_1^4 \quad \text{(A.7)}$$

$$S_{16}^{(1)} = \beta_1/2 + \beta_1^2/2 - 13\beta_1^3 + 34\beta_1^4 - 33\beta_1^5 + 11\beta_1^6 \quad \text{(A.8)}$$

$$S_{18}^{(1)} = \beta_1^2/4 - 3/2\beta_1^3 + 3/2\beta_1^4 + 4\beta_1^5 - 19/2\beta_1^6 + 7\beta_1^7 - 7/4\beta_1^8 \quad \text{(A.9)}$$

$$S_{20}^{(1)} = 16 \quad \text{(A.10)}$$

$$S_{22}^{(1)} = 32\beta_1 - 32\beta_1^2 \tag{A.11}$$

$$S_{24}^{(1)} = 8\beta_1 - 16\beta_1^3 + 8\beta_1^4 \tag{A.12}$$

$$S_{26}^{(1)} = 8\beta_1^2 - 24\beta_1^3 + 32\beta_1^4 - 24\beta_1^5 + 8\beta_1^6 \tag{A.13}$$

$$S_{28}^{(1)} = \beta_1^2 - 4\beta_1^3 + 8\beta_1^4 - 10\beta_1^5 + 8\beta_1^6 - 4\beta_1^7 + \beta_1^8 \tag{A.14}$$

The second harmonic solutions from the one-layer formulations are

$$A^{(2)} = \frac{k\left(N^0 + N^1kd + N^2k^2d^2 + N^3k^3d^3 + N^4k^4d^4 + N^5k^5d^5 + N^6k^6d^6\right)}{8\left[-dgk^2 - (1-\beta_1)\beta_1 2d^3gk^4 + \omega^2 + 2k^2d^2\omega^2 - 4(1-\beta_1)^2\beta_1^2k^4d^4\omega^2\right]} \tag{A.15}$$

$$U_1^{(2)} = \frac{k\left[1 + 2k^2d^2(1-\beta_1)^2\right]}{8} \cdot \frac{2\omega\left(U^{(1)2} + W^{(1)2}\right) + A^{(1)}\left[gk\left(4U^{(1)} - 4\beta_1kdW^{(1)} + \beta_1^2k^2d^2U^{(1)}\right) + 4\omega^2\left(W^{(1)} - \beta_1kdU^{(1)}\right)\right]}{-dgk^2 + 2(1-\beta_1)\beta_1d^3gk^4 + \omega^2 + 2k^2d^2\omega^2 + 4(1-\beta_1)^2\beta_1^2k^4d^4\omega^2}$$

(A.16)

$$W_1^{(2)} = \frac{dk^2(1-\beta_1)}{4} \cdot \frac{2\omega\left(U^{(1)2} - W^{(1)2}\right) + gkA^{(1)}\left(4U^{(1)} - 4\beta_1kdW^{(1)} + \beta_1^2k^2d^2U^{(1)}\right) + 4\omega^2\left(W^{(1)} - \beta_1kdU^{(1)}\right)}{-dgk^2 - 2(1-\beta_1)\beta_1d^3gk^4 + \omega^2 + 2k^2d^2\omega^2 - 4(1-\beta_1)^2\beta_1^2k^4d^4\omega^2}$$

(A.17)

$$Q_1^{(2)} = \frac{-\rho\omega}{4}\left\{\begin{array}{l} 2k^2d^2\left(U^{(1)2} - W^{(1)2}\right)\beta_1\left[2 + \left(-1 + 2k^2d^2\right)\beta_1 + \left(2\beta_1^3 - 4\beta_1^2\right)k^2d^2\right]\omega \\ +4\beta_1d^3k^3 \cdot \left[gk\left(1 - 3\beta_1 + \beta_1^2\right) - 4k^4d^3g + 4k^2d^2(1-\beta_1)^2\omega^2\right]W^{(1)}A^{(1)} \\ +\left[2d^6gk^7(1-\beta_1)^2\beta_1^4 + d^4gk^5\left(4 - 10\beta_1 + 7\beta_1^2\right)\beta_1^2\right]U^{(1)}A^{(1)} \\ +4\beta_1d^3k^3 \cdot \left[2\beta_1k^3d^2\left(3g - 2\beta_1g - 2d\omega^2\right) + (-1+\beta_1)^2\omega^2\right]U^{(1)}A^{(1)} \\ -\left[8d^5gk^6(-1+\beta_1)^2\beta_1^3 + 2\omega^2\right]W^{(1)}A^{(1)} \end{array}\right\}$$
$$\div\left[-dgk^2 - 2(1-\beta_1)\beta_1d^3gk^4 + \omega^2 + 2k^2d^2\omega^2 - 4(1-\beta_1)^2\beta_1^2k^4d^4\omega^2\right]$$

(A.18)

where

$$N^0 = 4A^{(1)}U^{(1)}\omega \tag{A.19}$$

$$N^1 = 2\left[U^{(1)2} - W^{(1)}\left(W^{(1)} + A^{(1)}(-2 + 2\beta_1)\omega\right)\right] \tag{A.20}$$

$$N^2 = A^{(1)}U^{(1)}\left(8-4\beta_1+\beta_1^2\right)\omega \tag{A.21}$$

$$N^3 = -4\beta_1\left[U^{(1)2}\left(-1+\beta_1\right)+W^{(1)}\left(W^{(1)}-W^{(1)}\beta_1+2A^{(1)}\beta_1\omega\right)\right] \tag{A.22}$$

$$N^4 = 2A^{(1)}U^{(1)}\beta_1^2\left(5+8\beta_1^2-12\beta_1\right)\omega \tag{A.23}$$

$$N^5 = -12A^{(1)}W^{(1)}\left(-1+\beta_1\right)^2\beta_1^3\omega \tag{A.24}$$

$$N^6 = 4A^{(1)}U^{(1)}\left(-1+\beta_1\right)\beta_1^4\omega \tag{A.25}$$

The third-order wave amplitude for one-layer formulations is

$$A^{(3)} = \frac{k\left(M^0+M^1kd+M^2k^2d^2+M^3k^3d^3+M^4k^4d^4+M^5k^5d^5+M^6k^6d^6\right)}{24\left[-4dgk^2-18\left(1-\beta_1\right)\beta_1d^3gk^4+4\omega^2+18k^2d^2\omega^2-81\left(1-\beta_1\right)^2\beta_1^2k^4d^4\omega^2\right]}$$

(A.26)

where

$$M^0 = 12\left[4A^{(2)}U^{(1)}+A^{(1)}\left(4U^{(2)}-kA^{(1)}W^{(1)}\right)\right]\omega \tag{A.27}$$

$$\begin{aligned} M^1 = {} & 4U^{(1)}\left[12U^{(2)}+A^{(1)2}k\left(-3+2\beta_1\right)\omega\right] \\ & +48\left\{2A^{(1)}W^{(2)}\left(1-\beta_1\right)\omega-W^{(1)}\left[W^{(2)}+\left(1-\beta_1\right)\omega A^{(2)}\right]\right\} \end{aligned} \tag{A.28}$$

$$\begin{aligned} M^2 = {} & -54k\omega A^{(1)2}W^{(1)}-8U^{(1)}\left[6\beta_1W^{(2)}+A^{(2)}\left(-27+6\beta_1-2\beta_1^2\right)\omega\right] \\ & +8U^{(2)}\left[6\beta_1W^{(1)}+A^{(1)}\left(27-24\beta_1+4\beta_1^2\right)\omega\right] \end{aligned} \tag{A.29}$$

$$\begin{aligned} M^3 = {} & 6\beta_1U^{(1)}\left[-4U^{(2)}\left(-9+8\beta_1\right)+3kA^{(1)2}\left(-1+3\beta_1\right)\omega\right]- \\ & 24\beta_1\left[18\beta_1\omega A^{(1)}W^{(2)}+W^{(1)}\left(9W^{(2)}-8\beta_1W^{(2)}+9\beta_1\omega A^{(2)}\right)\right] \end{aligned} \tag{A.30}$$

$$\begin{aligned} M^4 = {} & -36\beta_1^2U^{(2)}\left[6W^{(1)}\left(-1+\beta_1\right)+A^{(1)}\left(-7+30\beta_1-27\beta_1^2\right)\omega\right] \\ & +36\beta_1^2U^{(1)}\left[6\left(-1+\beta_1\right)W^{(2)}+A^{(2)}\left(23-48\beta_1+27\beta_1^2\right)\omega\right]-243\beta_1^2kA^{(1)2}W^{(1)}\left(1-\beta_1\right)^2\omega \end{aligned}$$

(1.31)

$$\begin{aligned} M^5 = {} & 54\left(1-\beta_1\right)\beta_1^3U^{(1)}\left[2U^{(2)}+3A^{(1)2}k\left(1-\beta_1\right)\omega\right]- \\ & 108\left(1-\beta_1\right)\beta_1^3\left\{18A^{(1)}W^{(2)}\left(1-\beta_1\right)\omega+W^{(1)}\left[W^{(2)}+9A^{(2)}\left(1-\beta_1\right)\omega\right]\right\} \end{aligned} \tag{A.32}$$

$$M^6 = 324\left(A^{(2)}U^{(1)}+2A^{(1)}U^{(2)}\right)\left(1-\beta_1\right)^2\beta_1^4\omega \tag{A.33}$$

APPENDIX B.

The dispersion relationship for the two-layer system is

$$\frac{\omega^2}{gk} = \frac{m_{11}^{(2)} dk + m_{13}^{(2)} k^3 d^3 + m_{15}^{(2)} k^5 d^5 + m_{17}^{(2)} k^7 d^7}{m_{20}^{(2)} + m_{22}^{(2)} d^2 k^2 + m_{24}^{(2)} k^4 d^4 + m_{26}^{(2)} k^6 d^6 + m_{28}^{(2)} k^8 d^8} \tag{B.1}$$

where

$$m_{11}^{(2)} = 1 \tag{B.2}$$

$$m_{13}^{(2)} = \frac{1}{2}\left[\beta_1 - \alpha_1^2 \beta_1 + \left(-1 + \alpha_1\right)\beta_1^2 + \alpha_1\left(\alpha_1 - \beta_2\right)\beta_2\right] \tag{B.3}$$

$$m_{15}^{(2)} = \frac{1}{4}\left\{\begin{aligned} &\beta_2^4 + \alpha_1^4\left(1 - \beta_1 + \beta_2\right) + \alpha_1^2\left(-\beta_1 + 3\beta_1^2 - 2\beta_1^3 + \beta_2 + 3\beta_2^2 + 2\beta_2^3\right) \\ &+2\alpha_1^3\left[-\beta_1 + \beta_1^2 - \beta_2\left(1 + \beta_2\right)\right] + \alpha_1\left[\beta_1^2 - 2\beta_1^3 + \beta_1^4 - \beta_2^2\left(1 + \beta_2\right)^2\right] \end{aligned}\right\} \tag{B.4}$$

$$m_{17}^{(2)} = -\frac{1}{8}\left(\alpha_1 - \beta_1\right)\left(-1 + \beta_1\right)\left(\alpha_1 - \beta_2\right)\beta_2 \left[\begin{aligned} &\beta_2^2 + \alpha_1^2\left(1 - \beta_1 + \beta_2\right) + \\ &\alpha_1\left[-\beta_1 + \beta_1^2 - \beta_2\left(1 + \beta_2\right)\right] \end{aligned}\right] \tag{B.5}$$

$$m_{20}^{(2)} = 1 \tag{B.6}$$

$$m_{22}^{(2)} = \frac{1}{2} \tag{B.7}$$

$$m_{24}^{(2)} = \frac{1}{4}\left\{\begin{aligned} &\alpha_1^4 + \beta_1^2 - 2\beta_1^3 + \beta_1^4 + \beta_2^4 - 2\alpha_1^3\left(\beta_1 + \beta_2\right) \\ &-2\alpha_1\left(-\beta_1^2 + \beta_1^3 + \beta_2^2 + \beta_2^3\right) + \alpha_1^2\left[-2\beta_1 + 3\beta_1^2 + \beta_2\left(2 + 3\beta_2\right)\right] \end{aligned}\right\} \tag{B.8}$$

$$m_{26}^{(2)} = \frac{1}{8}\left[\alpha_1^2\left(-1 + \beta_1 - \beta_2\right) - \beta_2^2 + \alpha_1\left(\beta_1 - \beta_1^2 + \beta_2 + \beta_2^2\right)\right]^2 \tag{B.9}$$

$$m_{28}^{(2)} = \frac{1}{16}\left(\alpha_1 - \beta_1\right)^2\left(1 - \beta_1\right)^2\left(\alpha_1 - \beta_2\right)^2\beta_2^2 \tag{B.10}$$

Velocities for the two-layer system are

$$w_1^{(1)} = \frac{gkA_1}{\omega_0}\frac{kd\left(\Lambda_{10}^{w1} + \Lambda_{11}^{w1} kd\right)}{\Lambda_{20}^{w1} + \Lambda_{22}^{w1} k^2 d^2 + \Lambda_{24}^{w1} k^4 d^4 + \Lambda_{26}^{w1} k^6 d^6 + \Lambda_{28}^{w1} k^8 d^8} \tag{B.11}$$

$$w_2^{(1)} = \frac{gkA_1}{\omega_0}\frac{kd\left(\Lambda_{10}^{w2} - \Lambda_{12}^{w2} k^2 d^2 + \Lambda_{14}^{w2} k^4 d^4\right)}{\Lambda_{20}^{w2} + \Lambda_{22}^{w2} k^2 d^2 + \Lambda_{24}^{w2} k^4 d^4 + \Lambda_{26}^{w2} k^6 d^6 + \Lambda_{28}^{w2} k^8 d^8} \tag{B.12}$$

$$u_1^{(1)} = \frac{gkA_1}{\omega_0}\frac{\Lambda_{10}^{u1} + \Lambda_{12}^{u1} k^2 d^2 + \Lambda_{14}^{u1} k^4 d^4 + \Lambda_{16}^{u1} k^6 d^6}{\Lambda_{20}^{u1} + \Lambda_{22}^{u1} k^2 d^2 + \Lambda_{24}^{u1} k^4 d^4 + \Lambda_{26}^{u1} k^6 d^6 + \Lambda_{28}^{u1} k^8 d^8} \tag{B.13}$$

$$u_2^{(1)} = \frac{gkA_1}{\omega_0} \frac{\Lambda_{10}^{u2} + \Lambda_{12}^{u2} k^2 d^2 + \Lambda_{14}^{u2} k^4 d^4 + \Lambda_{16}^{u2} k^6 d^6}{\Lambda_{20}^{u2} + \Lambda_{22}^{u2} k^2 d^2 + \Lambda_{24}^{u2} k^4 d^4 + \Lambda_{26}^{u2} k^6 d^6 + \Lambda_{28}^{u2} k^8 d^8} \tag{B.14}$$

where

$$\Lambda_{10}^{w1} = 16\left(-1+\beta_1\right) \tag{B.15}$$

$$\Lambda_{11}^{w1} = 4\left(-1+\beta_1\right)\left(\alpha_1-\beta_2\right)^4 \tag{B.16}$$

$$\Lambda_{20}^{w1} = 16 \tag{B.17}$$

$$\Lambda_{22}^{w1} = 8 \tag{B.18}$$

$$\Lambda_{24}^{w1} = 4\left\{\begin{aligned} &\alpha_1^4 - 2\alpha_1^3\left(\beta_1+\beta_2\right) + \beta_2^4 - 2\alpha_1\left(-\beta_1^2+\beta_1^3+\beta_2^2+\beta_2^3\right) \\ &+\beta_1^2 - 2\beta_1^3 + \beta_1^4 + \alpha_1^2\left[-2\beta_1 + 3\beta_1^2 + \beta_2\left(2+3\beta_2\right)\right] \end{aligned}\right\} \tag{B.19}$$

$$\Lambda_{26}^{w1} = 2\left[\alpha_1^2\left(-1+\beta_1-\beta_2\right) - \beta_2^2 + \alpha_1\left(\beta_1-\beta_1^2+\beta_2-\beta_2^2\right)\right]^2 \tag{B.20}$$

$$\Lambda_{28}^{w1} = \left[\left(\alpha_1-\beta_1\right)\beta_2\left(1-\beta_1\right)\left(\alpha_1-\beta_2\right)\right]^2 \tag{B.21}$$

$$\Lambda_{10}^{w2} = 16\left(-1+\beta_2\right) \tag{B.22}$$

$$\Lambda_{12}^{w2} = 8\left(-1+\alpha_1\right)\left(\beta_1-\beta_2\right)\left(-1-\alpha_1+\beta_1+\beta_2\right) \tag{B.23}$$

$$\Lambda_{14}^{w2} = 4\left(\alpha_1-\beta_1\right)\left(1-\beta_1\right)\left(\alpha_1-\beta_2\right)\left[\alpha_1^2 - \beta_1 + \beta_1^2 + \beta_2 - \alpha_1\left(\beta_1+\beta_2\right)\right] \tag{B.24}$$

$$\Lambda_{20}^{w2} = 16 \tag{B.25}$$

$$\Lambda_{22}^{w2} = 8 \tag{B.26}$$

$$\Lambda_{24}^{w2} = 4\left\{\begin{aligned} &\alpha_1^4 + \beta_1^2 - 2\alpha_1^3\left(\beta_1+\beta_2\right) - 2\alpha_1\left(-\beta_1^2+\beta_1^3+\beta_2^2+\beta_2^3\right) \\ &-2\beta_1^3 + \beta_1^4 + \beta_2^4 + \alpha_1^2\left[-2\beta_1 + 3\beta_1^2 + \beta_2\left(2+3\beta_2\right)\right] \end{aligned}\right\} \tag{B.27}$$

$$\Lambda_{26}^{w2} = 2\left[\alpha_1^2\left(-1+\beta_1-\beta_2\right) - \beta_2^2 + \alpha_1\left(\beta_1-\beta_1^2+\beta_2-\beta_2^2\right)\right]^2 \tag{B.28}$$

$$\Lambda_{28}^{w2} = \beta_2^2\left(\alpha_1-\beta_1\right)^2\left(1-\beta_1\right)^2\left(\alpha_1-\beta_2\right)^2 \tag{B.29}$$

$$\Lambda_{10}^{u1} = 16 \tag{B.30}$$

$$\Lambda_{12}^{u1} = 8\left(1-\beta_1\right)^2 \tag{B.31}$$

$$\Lambda_{14}^{u1} = 4\left(\alpha_1-\beta_2\right)^2 \tag{B.32}$$

$$\Lambda_{16}^{u1} = 2\left(1-\beta_1\right)^2\left(\alpha_1-\beta_2\right)^4 \tag{B.33}$$

$$\Lambda_{20}^{u1} = 16 \tag{B.34}$$

$$\Lambda_{22}^{u1} = 8 \tag{B.35}$$

$$\Lambda_{24}^{u1} = 4\left\{\begin{array}{l} \alpha_1^4 - 2\beta_1^3 + \beta_2^4 + \alpha_1^2\left[-2\beta_1 + 3\beta_1^2 + \beta_2\left(2+3\beta_2\right)\right] \\ +\beta_1^2 + \beta_1^4 - 2\alpha_1^3\left(\beta_1+\beta_2\right) - 2\alpha_1\left(-\beta_1^2 + \beta_1^3 + \beta_2^2 + \beta_2^3\right) \end{array}\right\} \tag{B.36}$$

$$\Lambda_{26}^{u1} = 2\left[\alpha_1^2\left(-1+\beta_1-\beta_2\right) - \beta_2^2 + \alpha_1\left(\beta_1 - \beta_1^2 + \beta_2 - \beta_2^2\right)\right]^2 \tag{B.37}$$

$$\Lambda_{28}^{u1} = \beta_2^2\left(\alpha_1-\beta_1\right)^2\left(1-\beta_1\right)^2\left(\alpha_1-\beta_2\right)^2 \tag{B.38}$$

$$\Lambda_{10}^{u2} = 16 \tag{B.39}$$

$$\Lambda_{12}^{u2} = 8\left(1-\beta_2\right)^2 \tag{B.40}$$

$$\Lambda_{14}^{u2} = 4\left[\alpha_1^2 - \beta_1 + \beta_1^2 + \beta_2 - \alpha_1\left(\beta_1+\beta_2\right)\right]^2 \tag{B.41}$$

$$\Lambda_{16}^{u2} = 2\left[\left(\alpha_1-\beta_1\right)\left(1-\beta_1\right)\left(\alpha_1-\beta_2\right)\right]^2 \tag{B.42}$$

$$\Lambda_{20}^{u2} = 16 \tag{B.43}$$

$$\Lambda_{22}^{u2} = 8 \tag{B.44}$$

$$\Lambda_{24}^{u2} = 4\left\{\begin{array}{l} \alpha_1^4 + \beta_1^2 - 2\beta_1^3 + \alpha_1^2\left[-2\beta_1 + 3\beta_1^2 + \beta_2\left(2+3\beta_2\right)\right] \\ +\beta_1^4 + \beta_2^4 - 2\alpha_1^3\left(\beta_1+\beta_2\right) + 2\alpha_1\left(\beta_1^2 - \beta_1^3 - \beta_2^2 - \beta_2^3\right) \end{array}\right\} \tag{B.45}$$

$$\Lambda_{26}^{u2} = 2\left[\alpha_1^2\left(-1+\beta_1-\beta_2\right) - \beta_2^2 + \alpha_1\left(\beta_1 - \beta_1^2 + \beta_2 - \beta_2^2\right)\right]^2 \tag{B.46}$$

$$\Lambda_{28}^{u2} = \beta_2^2\left(\alpha_1-\beta_1\right)^2\left(1-\beta_1\right)^2\left(\alpha_1-\beta_2\right)^2 \tag{B.47}$$

The shoaling coefficient for the two-layer system is

$$s = \frac{S_{10}^{(2)} + S_{12}^{(2)}k^2d^2 + S_{14}^{(2)}k^4d^4 + S_{16}^{(2)}k^6d^6 + \mathrm{O}\left(k^8d^8\right)}{S_{20}^{(2)} + S_{22}^{(2)}k^2d^2 + S_{24}^{(2)}k^4d^4 + S_{26}^{(2)}k^6d^6 + \mathrm{O}\left(k^8d^8\right)} \tag{B.48}$$

where

$$S_{10}^{(2)} = -4 \tag{B.49}$$

1 $$S_{12}^{(2)} = 4\left[1-6\beta_1\left(1-\alpha_1^2\right)+6\left(1-\alpha_1\right)\beta_1^2-6\alpha_1^2\beta_2+6\alpha_1\beta_2^2\right] \tag{B.50}$$

2 $$S_{14}^{(2)} = \left\{\begin{array}{l} 3+3\beta_1-43\beta_1^2+80\beta_1^3-40\beta_1^4-10\beta_2^4 \\ -\alpha_1^2\left[\begin{array}{l} 60\beta_1^3+51\beta_1^4-6\beta_1^2\left(12+17\beta_2+17\beta_2^2\right) \\ +2\beta_1\left(2+51\beta_2\right)+\beta_2\left(-4+30\beta_2+42\beta_2^2+51\beta_2^3\right) \end{array}\right]- \\ \alpha_1\left[82\beta_1^3-81\beta_1^4-102\beta_1\beta_2^2-\beta_1^2\left(4-102\beta_2^2\right)-\beta_2^2\left(4-20\beta_2-21\beta_2^2\right)\right] \\ -\alpha_1^4\left[10+51\beta_1^2+21\beta_2+51\beta_2^2-3\beta_1\left(7+34\beta_2\right)\right]+ \\ 2\alpha_1^3\left[51\beta_1^3-3\beta_1^2\left(7+17\beta_2\right)+\beta_1\left(10-51\beta_2^2\right)+\beta_2\left(10+21\beta_2+51\beta_2^2\right)\right] \end{array}\right\} \tag{B.51}$$

3 $$S_{16}^{(2)} = \left\{\begin{array}{l} -12\beta_1^3+56\beta_1^4-60\beta_1^6+10\beta_2^4+\beta_1\left(7-60\beta_2^4\right)+\beta_1^2\left(-11+60\beta_2^4\right)- \\ 3\alpha_1^5\left[\begin{array}{l} 55\beta_1^4-2\beta_1^3\left(39+55\beta_2\right)+2\beta_1\beta_2^2\left(39+55\beta_2\right) \\ +\beta_1^2\left(43+79\beta_2\right)-\beta_2^2\left(43+78\beta_2+55\beta_2^2\right) \end{array}\right]+ \\ \alpha_1^6\left[\begin{array}{l} 55\beta_1^3-\beta_2\left(43+78\beta_2+55\beta_2^2\right)- \\ 3\beta_1^2\left(26+55\beta_2\right)+\beta_1\left(43+156\beta_2+165\beta_2^2\right) \end{array}\right]+ \\ \alpha_1\left[\begin{array}{l} 96\beta_1^5+\beta_1^4\left(-22+147\beta_2^2\right)+2\beta_1\beta_2^2\left(4+60\beta_2+39\beta_2^2\right) \\ -14\beta_1^3\left(2+21\beta_2^2\right)+\beta_1^2\left(13+139\beta_2^2-120\beta_2^3-138\beta_2^4\right) \\ -52\beta_1^6+\beta_2^2\left(-13-20\beta_2+3\beta_2^2+43\beta_2^4\right) \end{array}\right]+ \\ \alpha_1^4\left[\begin{array}{l} 10+165\beta_1^5-25\beta_2^2-215\beta_2^3-312\beta_2^4-2\beta_1^3\left(14+87\beta_2+\beta_2^2\right) \\ -3\beta_1^4\left(49+55\beta_2\right)+\beta_1^2\left(113+348\beta_2+477\beta_2^2+330\beta_2^3\right) \\ -3\beta_2-165\beta_2^5+\beta_1\left(-57-28\beta_2+105\beta_2^2+156\beta_2^3+165\beta_2^4\right) \end{array}\right]+ \\ \alpha_1^3\left[\begin{array}{l} +2\beta_1^3\left(-113-105\beta_2+87\beta_2^2\right)+\beta_1^4\left(271+252\beta_2+165\beta_2^2\right) \\ -96\beta_1^5+\beta_1\left(-20+120\beta_2+106\beta_2^2+210\beta_2^3-78\beta_2^4\right) \\ -55\beta_1^6-\beta_1^2\left(-114+170\beta_2+486\beta_2^2+486\beta_2^3+165\beta_2^4\right) \end{array}\right] \\ +\alpha_1^2\left[\begin{array}{l} \beta_1^4\left(17-147\beta_2-252\beta_2^2\right)+7\beta_1^3\left(-5+42\beta_2+30\beta_2^2\right) \\ +87\beta_1^6-105\beta_1^5-\beta_1\left(13+8\beta_2+180\beta_2^2+105\beta_2^4\right) \\ +\beta_1^2\left(38-139\beta_2+230\beta_2^2+276\beta_2^3+243\beta_2^4\right) \\ -\beta_2\left(-13-30\beta_2+6\beta_2^2+25\beta_2^3+129\beta_2^4+78\beta_2^5\right) \end{array}\right] \end{array}\right. \tag{B.52}$$

4 $$S_{20}^{(2)} = -16 \tag{B.53}$$

5 $$S_{22}^{(2)} = -8\left[1-9\beta_1\left(-1+\alpha_1^2\right)+9\left(-1+\alpha_1\right)\beta_1^2+9\beta_2\alpha_1^2-9\alpha_1\beta_2^2\right] \tag{B.54}$$

$$S_{24}^{(2)}=-4\left\{\begin{array}{l}11\beta_1+22\beta_1^2+33\beta_1^4+\alpha_1^4\left(10+34\beta_1^2+11\beta_2+34\beta_2^2-\beta_1\left(11+68\beta_2\right)\right)-\\ \alpha_1\left[-48\beta_1^3+57\beta_1^4+68\beta_1\beta_2^2+\beta_2^2\left(20+20\beta_2+11\beta_2^2\right)-4\beta_1^2\left(5+17\beta_2^2\right)\right]\\ -2\alpha_1^3\left[34\beta_1^3-\beta_1^2\left(11+34\beta_2\right)+\beta_1\left(10-34\beta_2^2\right)+\beta_2\left(10+11\beta_2+34\beta_2^2\right)\right]\\ +10\beta_2^4+\alpha_1^2\left[\begin{array}{l}46\beta_1^3+34\beta_1^4-2\beta_1^2\left(19+34\beta_2+34\beta_2^2\right)\\ +4\beta_1\left(-5+17\beta_2\right)+2\beta_2\left(10+15\beta_2+11\beta_2^2+17\beta_2^3\right)\end{array}\right]\end{array}\right\} \tag{B.55}$$

$$S_{26}^{(2)}=2\left\{\begin{array}{c}27\beta_1^3-195\beta_1^5+65\beta_1^6-10\beta_2^4-2\beta_1\left(1+45\beta_2^4\right)+\beta_1^2\left(-44+90\beta_2^4\right)\\ +149\beta_1^4-3\alpha_1^5\left[\begin{array}{l}70\beta_1^4-2\beta_1^3\left(41+70\beta_2\right)+2\beta_1\beta_2^2\left(41+70\beta_2\right)\\ +\beta_1^2\left(77+82\beta_2\right)-\beta_2^2\left(77+82\beta_2+70\beta_2^2\right)\end{array}\right]+\\ \alpha_1^6\left[\begin{array}{l}-2\beta_1^2\left(41+105\beta_2\right)-\beta_2\left(77+82\beta_2+70\beta_2^2\right)\\ +70\beta_1^3+\beta_1\left(77+164\beta_2+210\beta_2^2\right)\end{array}\right]+\\ \alpha_1^4\left[\begin{array}{l}-10+210\beta_1^5-22\beta_2-130\beta_2^2-385\beta_2^3+\beta_1^3\left(93-256\beta_2-420\beta_2^2\right)\\ -2\beta_1^4\left(59+105\beta_2\right)+\beta_1^2\left(42+412\beta_2+538\beta_2^2+420\beta_2^3\right)\\ -328\beta_2^4-210\beta_2^5+2\beta_1\left(-34+89\beta_2-60\beta_2^2+82\beta_2^3+105\beta_2^4\right)\end{array}\right]\\ +\alpha_1\left[\begin{array}{l}+2\beta_1\beta_2^2\left(81+90\beta_2+41\beta_2^2\right)+2\beta_1^4\left(51+109\beta_2^2\right)\\ +174\beta_1^5-123\beta_1^6-\beta_1^2\left(13-56\beta_2^2+180\beta_2^3+172\beta_2^4\right)\\ -2\beta_1^3\left(71+218\beta_2^2\right)+\beta_2^2\left(13+20\beta_2+22\beta_2^2+77\beta_2^4\right)\end{array}\right]\\ +\alpha_1^3\left[\begin{array}{l}+4\beta_1^3\left(-21-60\beta_2+64\beta_2^2\right)+\beta_1^4\left(199+338\beta_2+210\beta_2^2\right)\\ -174\beta_1^5+\beta_1\left(20+180\beta_2-96\beta_2^2+240\beta_2^3-82\beta_2^4\right)\\ -70\beta_1^6-2\beta_1^2\left(-68+220\beta_2+292\beta_2^2+292\beta_2^3+105\beta_2^4\right)\\ +\beta_2\left(20+44\beta_2+262\beta_2^2+385\beta_2^3+246\beta_2^4+70\beta_2^5\right)\end{array}\right]\\ +\alpha_1^2\left[\begin{array}{l}-15\beta_1^5-\beta_1\left(-13+162\beta_2+270\beta_2^2+164\beta_2^3+120\beta_2^4\right)\\ +128\beta_1^6-\beta_2\left(13+30\beta_2+44\beta_2^2+130\beta_2^3+231\beta_2^4+82\beta_2^5\right)\\ -2\beta_1^4\left(66+109\beta_2+169\beta_2^2\right)+2\beta_1^4\left(-85+218\beta_2+120\beta_2^2\right)\\ +2\beta_1^2\left(66-28\beta_2+265\beta_2^2+172\beta_2^3+146\beta_2^4\right)\end{array}\right]\end{array}\right\} \tag{B.56}$$

FIGURE CAPTIONS

Figure 1 Definition sketch. The water column is divided into N vertical layers by (N – 1) non-intersecting interfaces, and velocities and pressure are defined at an arbitrary elevation h_j within each vertical layer z_j.

Figure 2 Accuracy of the phase speed, group velocity and linear shoaling gradient for the one-layer formulation. they show a high degree of accuracy with Stokes theory over the range $kd \leq \pi$.

Figure 3 Vertical profiles of the horizontal velocity (top row) and vertical velocity (bottom row) for different kd. The present formulations yield a good agreement with the linear Stokes theory and have a higher degree of accuracy than the second-order Boussinesq theory.

Figure 4 Accuracy of the second and third-order nonlinear amplitudes from one-layer and Boussinesq models. The present solution obtains an overall good agreement with the Stokes second-order theory for $kd \leq \pi$, and yields much smaller maximum error than that predicted by the Boussinesq models derived by Nwogu (1993) and Wei et al. (1995) for the same range.

Figure 5 Accuracy of the phase speed, group velocity and linear shoaling gradient of the two-layer formulation. The formulation with partially optimized coefficients provides the most accurate solutions for the phase speed, group velocity and shoaling effect, and the uniform-layer formulation yields the closest phase speed but the most inaccurate group velocity and shoaling coefficient.

Figure 6 Vertical profiles of the horizontal velocity (top row) and vertical velocity (bottom row) for different kd. The formulation with optimized coefficients yields the most accurate results compared to Stokes theory over the range $kd \leq 4\pi$, and the two-uniform-layer mode also well represents the vertical velocity profiles with slight deviations at the medium water depth in the region with relative large water depth, while the formulation with partially optimized coefficients predicts completely wrong velocity profiles for large kd.

Figure 7 Accuracy of the second and third-order nonlinear wave amplitudes. The optimized coefficients lead to slight larger error than the uniform-layer solutions in the special range $\pi/4 \leq kd \leq 7\pi/4$ but obtain an overall higher degree of accuracy over the optimized range $0 < kd \leq 4\pi$.

Figure 8 Accuracy of the phase speed, group velocity and linear shoaling gradient for the three-layer formulation. The three-layer model with optimized coefficients exhibits more accurate characteristics than the uniform-layer model and performs consistently better than the one and two-layer models within its application range.

Figure 9 Vertical profiles of the horizontal velocity (top row) and vertical velocity (bottom row) for different kd. The three-layer model with optimized coefficients predicts the vertical velocity profiles to a much higher degree of accuracy than the three-uniform-layer model, and it can be able to provides satisfactory results in extremely deep water, e.g. up to $kd = 10\pi$.

Figure 10 Accuracy of the second and third-order nonlinear amplitudes. The three-layer model with optimized coefficients provides overall satisfactory second and third-order solutions than the three-uniform-layer model.

Figure 1

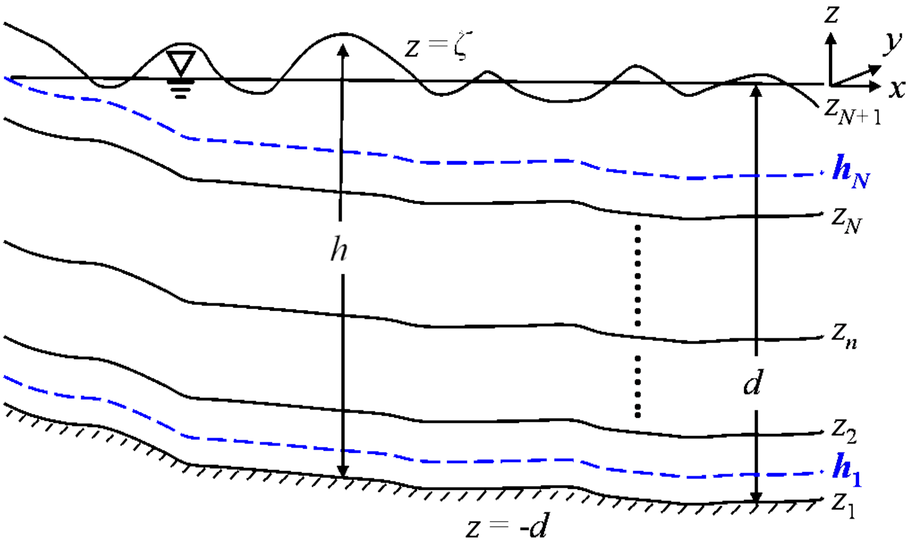

Figure 2

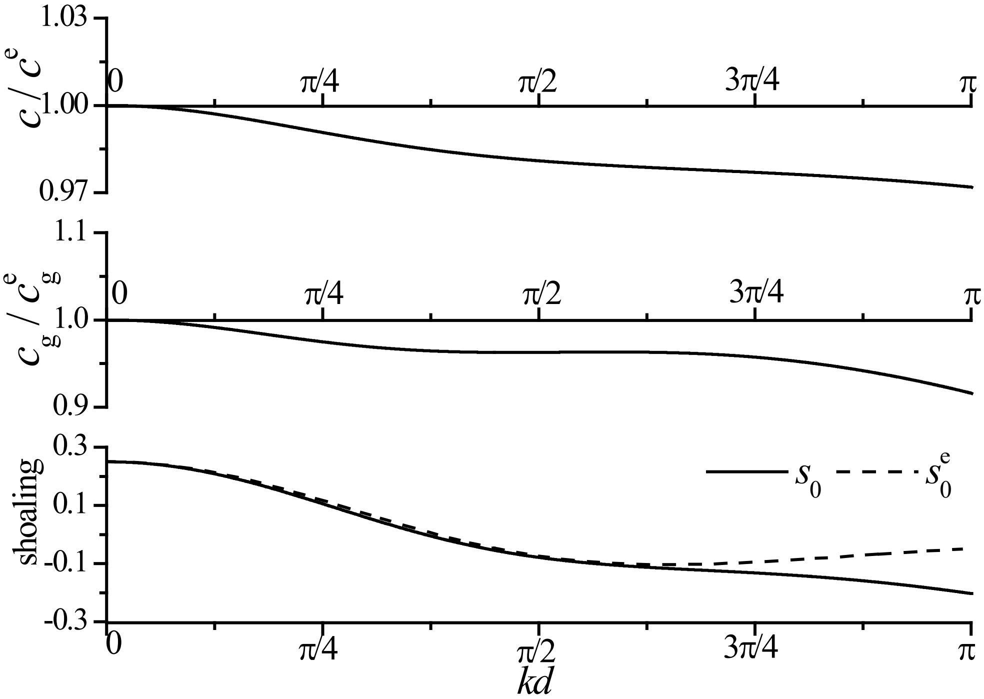
1.03
1.00
0.97
c / c^{e}
1.1
1.0
0.9
c_g / c_g^{e}
0.3
0.1
-0.1
-0.3
shoaling
s_0
s_0^{e}
0
π/4
π/2
3π/4
π
kd

Figure 3

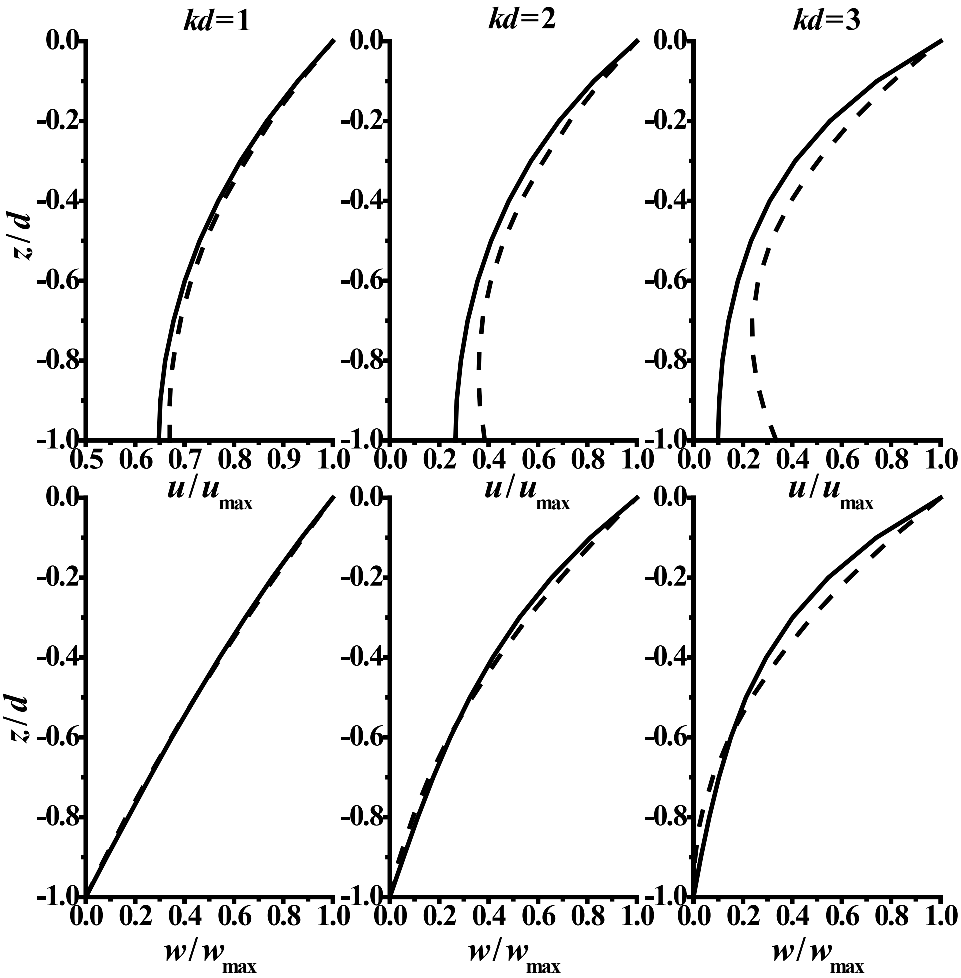
kd=1
kd=2
kd=3
0.0
-0.2
-0.4
-0.6
-0.8
-1.0
z/d
0.5 0.6 0.7 0.8 0.9 1.0
0.0 0.2 0.4 0.6 0.8 1.0
u/u max
w/w max

Figure 4

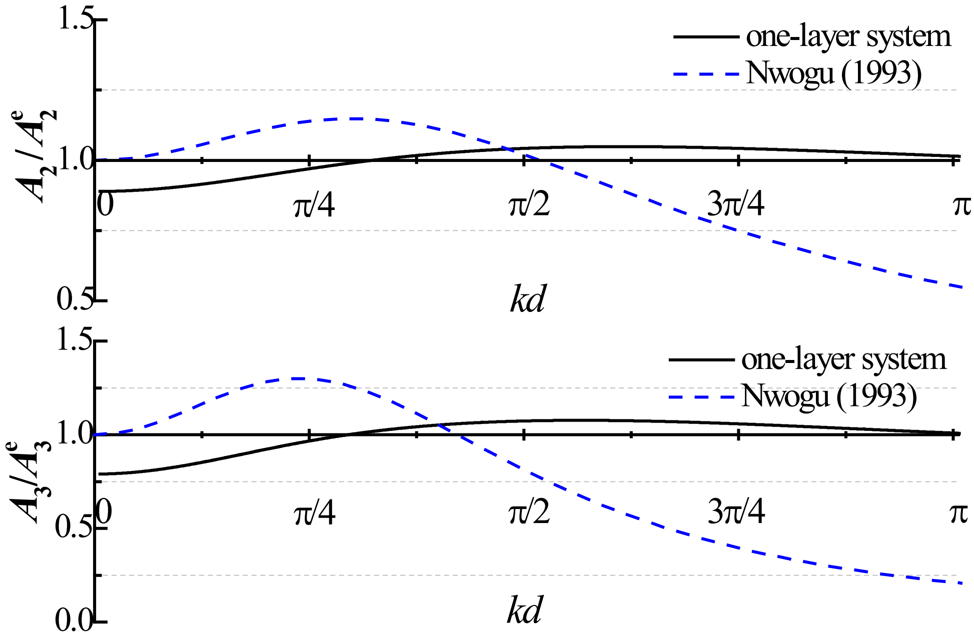
1.5
1.0
0.5
A_2/A_2^e
0
π/4
π/2
3π/4
π
kd
one-layer system
Nwogu (1993)
1.5
1.0
0.5
0.0
A_3/A_3^e
0
π/4
π/2
3π/4
π
kd
one-layer system
Nwogu (1993)

Figure 5

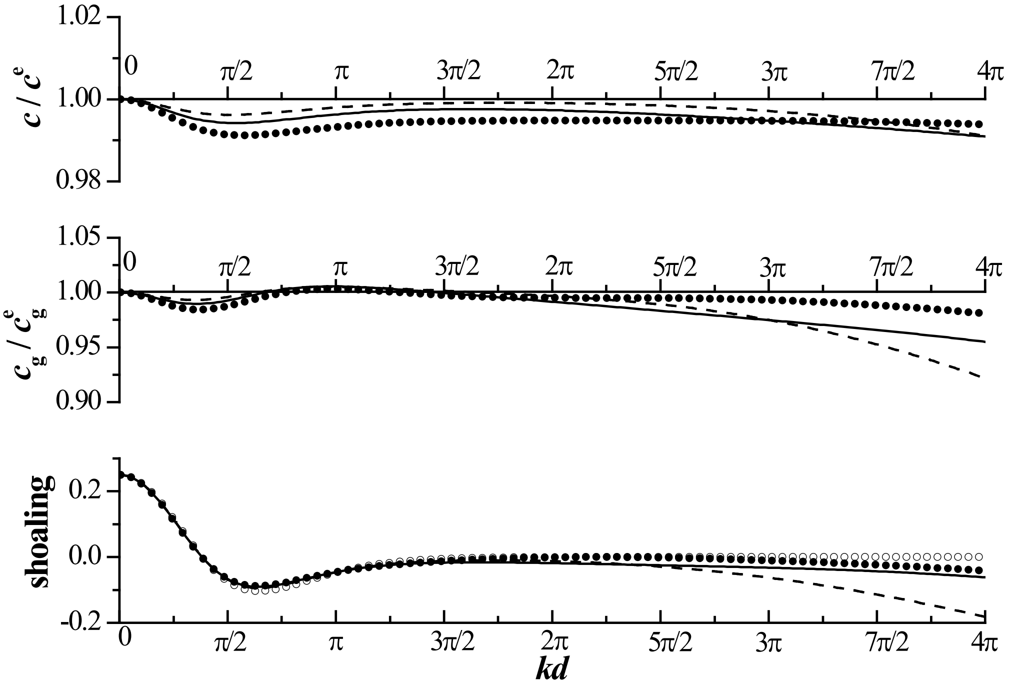
1.02
1.00
0.98
c / c^e
1.05
1.00
0.95
0.90
c_g / c_g^e
0.2
0.0
-0.2
shoaling
0
π/2
π
3π/2
2π
5π/2
3π
7π/2
4π
kd

Figure 6

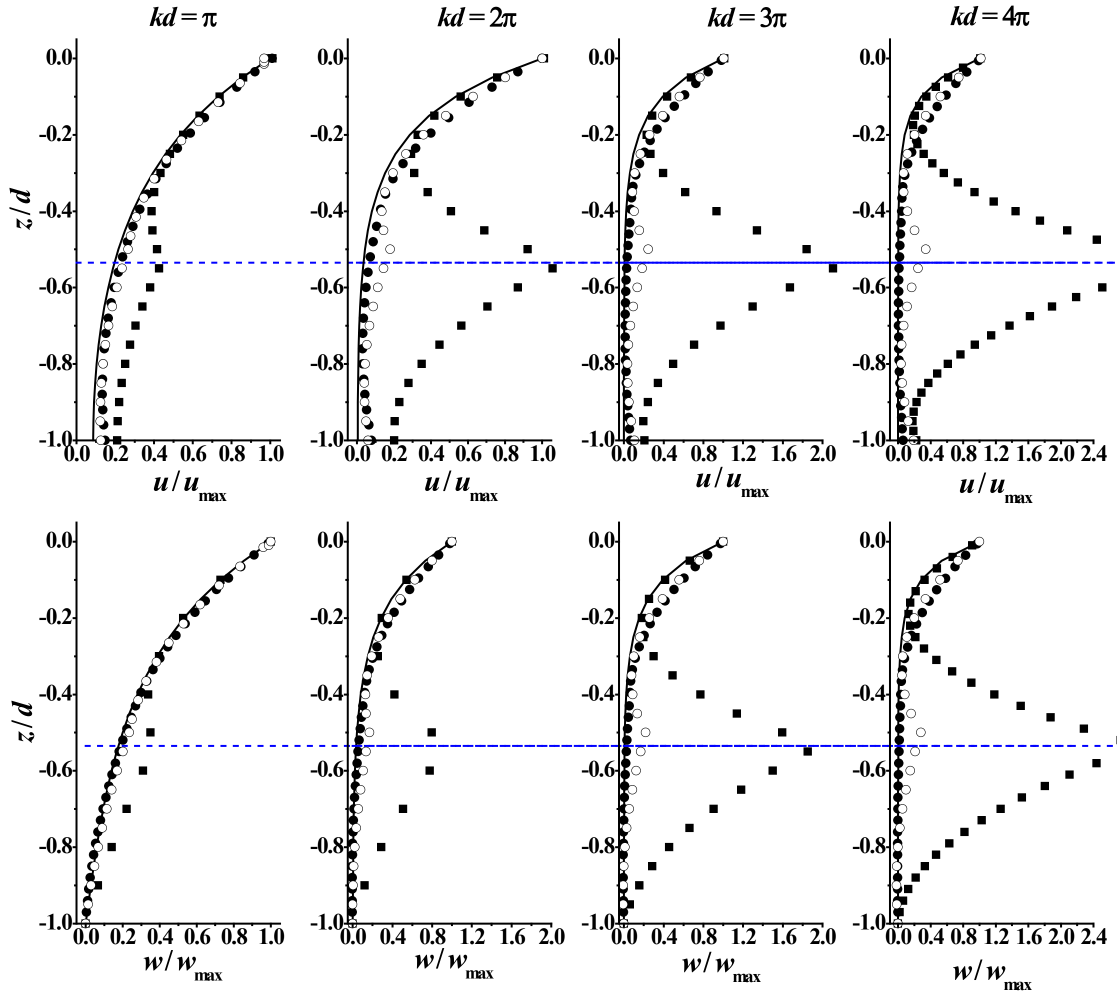

Figure 7

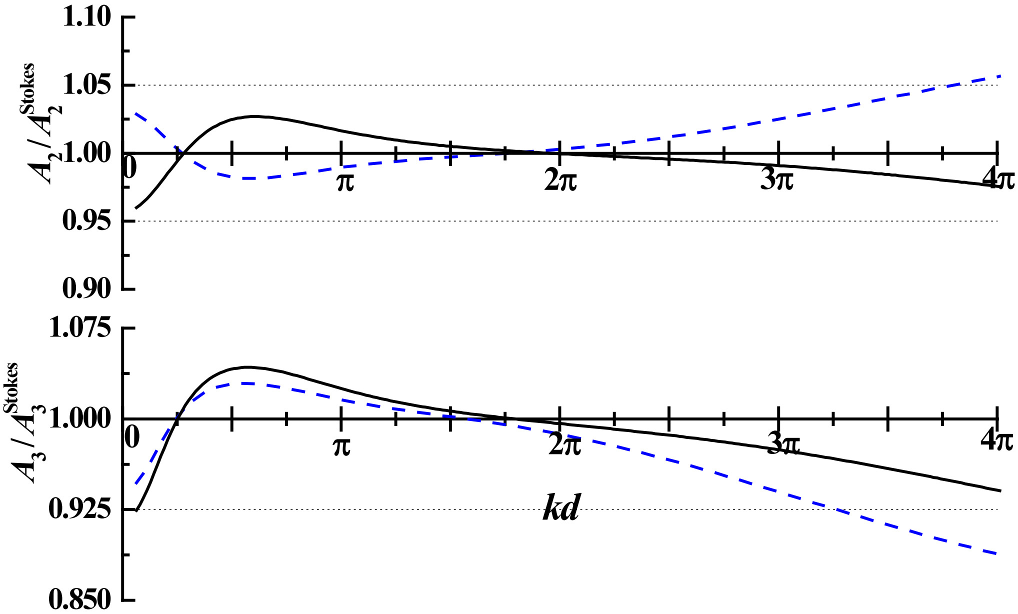
1.10
1.05
1.00
0.95
0.90
A_2 / A_2^{Stokes}
0
π
2π
3π
4π
1.075
1.000
0.925
0.850
A_3 / A_3^{Stokes}
kd

Figure 8

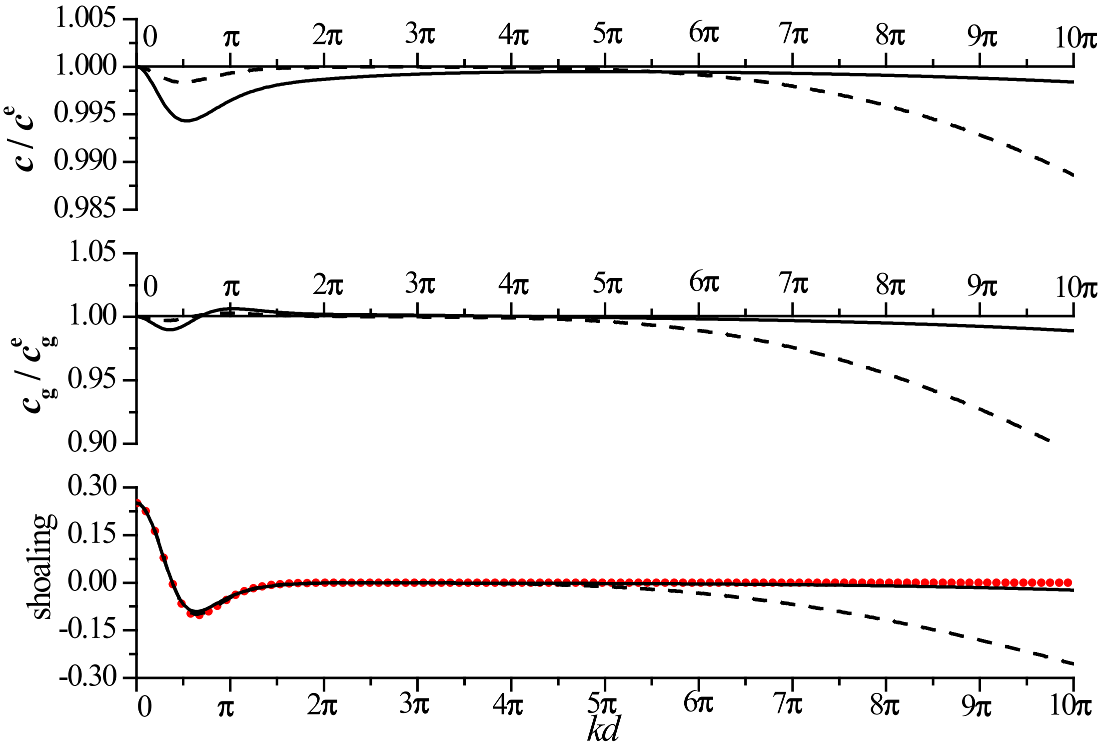
1.005
1.000
0.995
0.990
0.985
c / c^e
0
π
2π
3π
4π
5π
6π
7π
8π
9π
10π
1.05
1.00
0.95
0.90
c_g / c_g^e
0.30
0.15
0.00
-0.15
-0.30
shoaling
kd

Figure 9

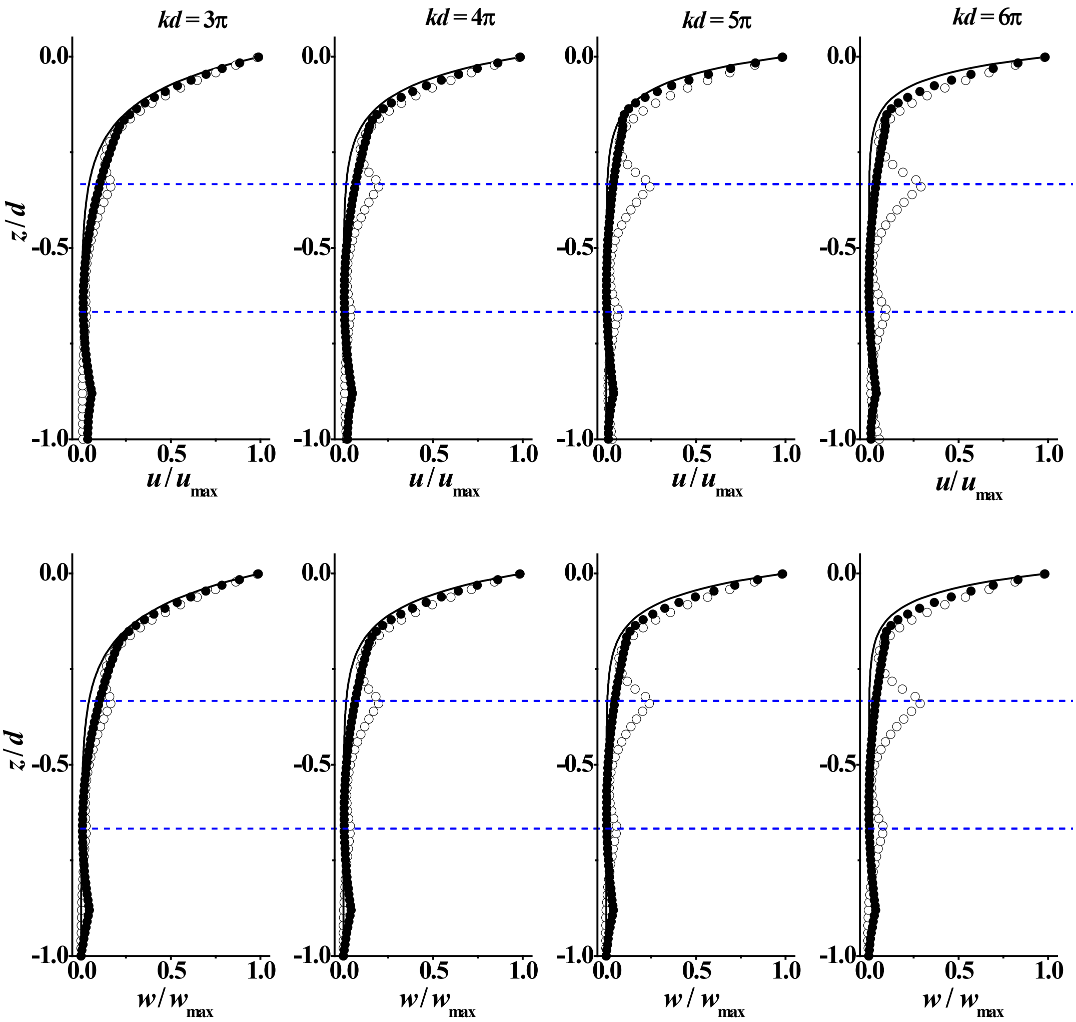

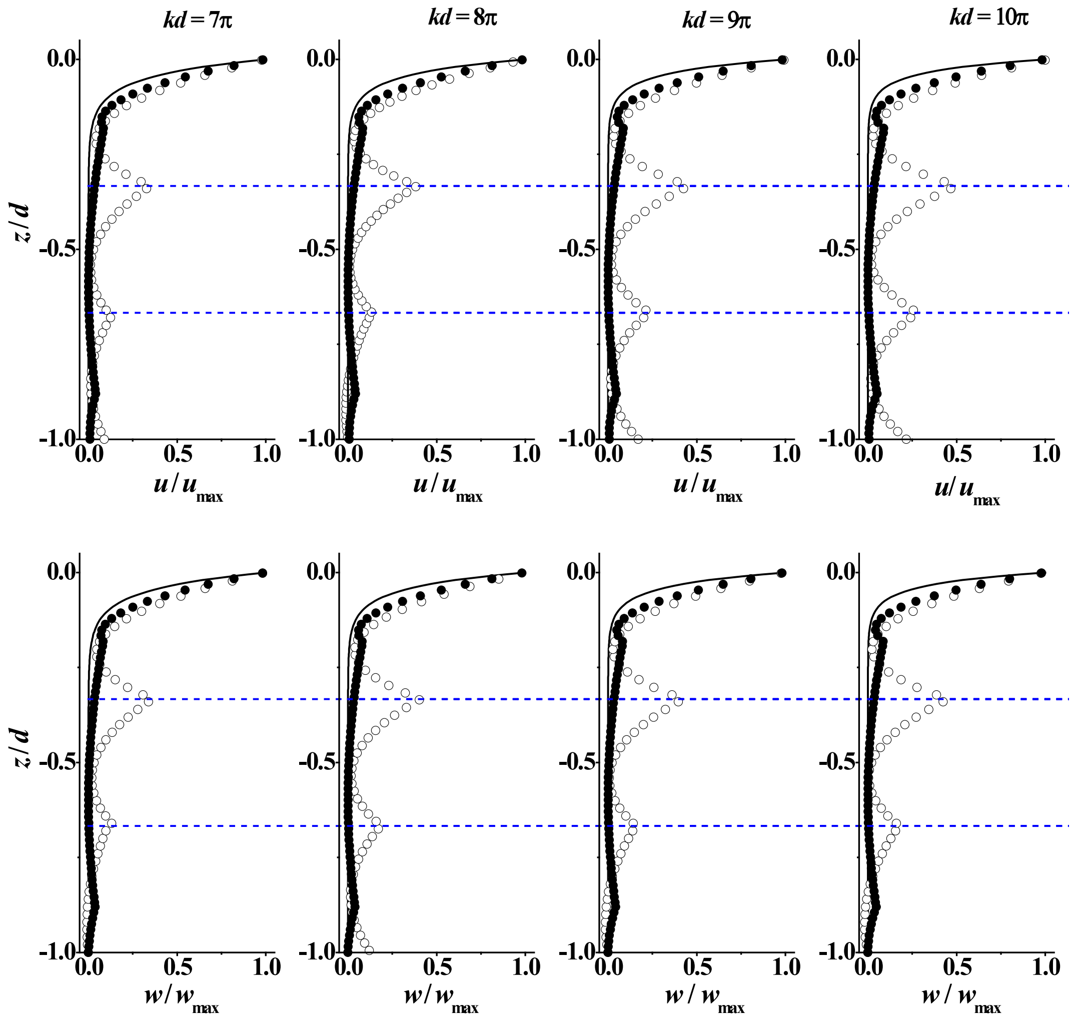

1

Figure 10

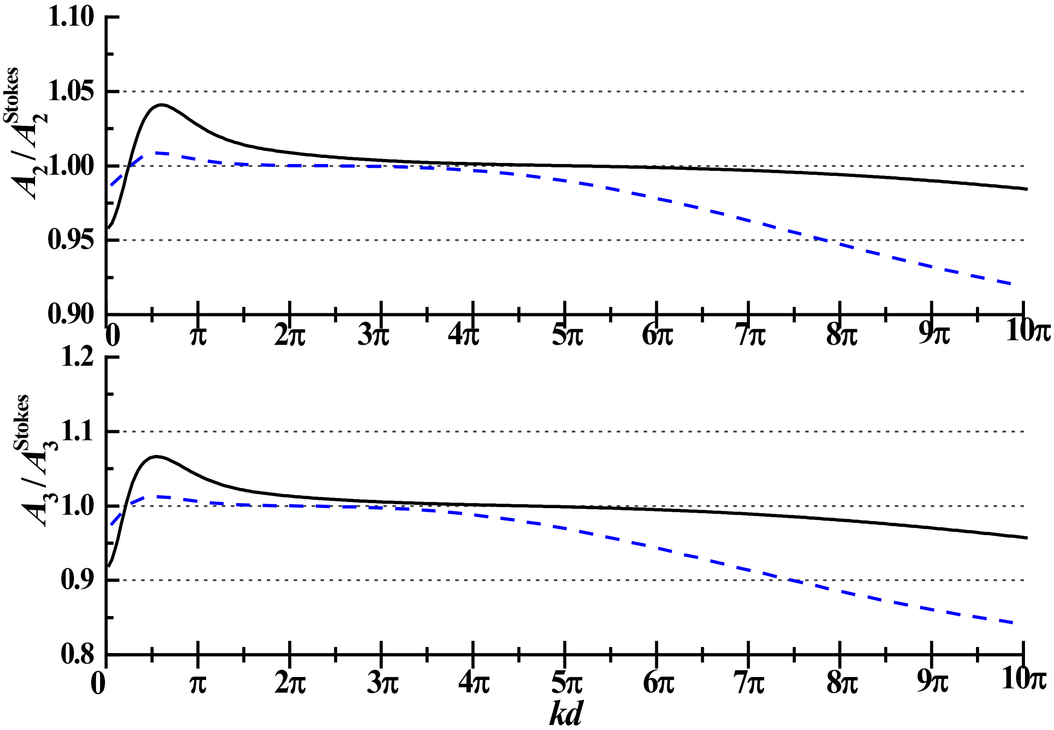
1.10
1.05
1.00
0.95
0.90
A_2 / A_2^{Stokes}
0
π
2π
3π
4π
5π
6π
7π
8π
9π
10π
1.2
1.1
1.0
0.9
0.8
A_3 / A_3^{Stokes}
kd